THE GEOLOGICAL SOCIETY OF AMERICA®

Jake Seller Draw impact structure, Bighorn Basin, Wyoming, USA: The deepest known buried impact structure on Earth and its possible relation to the Wyoming crater field

Sebastian Sturm[1,†], Thomas Kenkmann[1], Doug Cook[2], Allan Fraser[3], and Kent Sundell[4]
[1]*Institute of Earth and Environmental Sciences, Albert-Ludwigs-Universität Freiburg, Albertstraße 23B, 79104 Freiburg, Germany*
[2]*Independent consultant, Colorado Springs, Colorado 80904, USA*
[3]*Independent consultant, Casper, Wyoming 82609, USA*
[4]*School of Science, Casper College, Casper, Wyoming 82601, USA*

ABSTRACT

We provide evidence demonstrating the impact origin of a structure, here named the Jake Seller Draw impact structure, which is buried below the Jake Seller Draw drainage basin, in the Bighorn Basin of Wyoming, western United States. The 4.3-km-diameter structure was first recognized as a seismic disturbance at a depth of ∼6.5 km in two- and three-dimensional seismic profiles. Microstructural analysis of drill cuttings situated in the center and outside of Jake Seller Draw revealed the presence of multiple sets of planar deformation features and planar fractures in nine quartz grains, thereby confirming the hypervelocity impact origin of the structure. The seismic data show that Jake Seller Draw is a complex impact structure containing a 1-km-wide central uplift. The geologic and seismic data suggest that Jake Seller Draw is the most deeply buried impact structure known on Earth to date. The stratigraphic framework suggests that the crater was formed in a nearshore environment at the Pennsylvanian–Permian boundary, ∼280 m.y. ago. This age coincides with the age of the Wyoming crater field 300 km southeast of Jake Seller Draw and may suggest a common origin.

1. INTRODUCTION

Compared to the Moon or Mars, the number of impact craters discovered on Earth (currently 208 impact structures) is very low (Gottwald et al., 2020; Kenkmann, 2021). This paucity of discovered impact structures on Earth is caused by erosion, burial, tectonic deformation, and two-thirds of Earth's surface being covered with water, with young oceanic crust underneath most of this area. The discovery, analysis, and final confirmation of buried and/or marine impact structures on Earth are especially challenging because this type of investigation requires geophysical surveying and expensive drilling to collect samples with clear shock effects (e.g., planar deformation features; e.g., French and Koeberl, 2010). Buried craters are sometimes discovered during intensive subsurface surveying as part of economic exploration, mostly for hydrocarbons (e.g., Gulick et al., 2013; Kenkmann et al., 2015; Nicholson et al., 2022). About 21% (43) of the known impact craters on Earth are completely buried (Kenkmann, 2021). Previously, the Newporte structure, North Dakota, western United States (Koeberl and Reimold, 1995), with an overburden of ∼3 km, was the most deeply buried known impact structure on Earth.

Buried craters are commonly well preserved, although a phase of erosion in their postimpact geologic history could change this state. This preservation makes them important for scientific investigation. Craters can be deeply buried at places that were or became depocenters. In this context, a deeply buried crater is defined as one for which the overburden thickness is at least one-third of the crater detection limit depth, H, which is slightly deeper than the transient crater depth. The crater detection limit, H, represents a threshold, which is defined by the maximum depth, $H(D)$, down to which shock effects are recognizable for a given crater diameter, D. The crater detection limit is defined by: $-1/30H$ for shallowly buried, $-1/10H$ for moderately buried, and $-1/3H$ for deeply buried structures (Kenkmann, 2021). Additionally, based on the presence of reworked breccia or resurge deposits, marine or aquatic conditions during formation can be inferred, which has been documented for 33 impact structures so far (Kenkmann, 2021). These include the two large impact events into shallow-marine shelf environments: Chicxulub (Morgan et al., 2016) and Chesapeake Bay (Poag et al., 2004). In this context, the recently discovered Nadir structure, situated offshore of West Africa, represents a possible candidate for a well-preserved marine and buried crater, which is thought to have been formed at the Cretaceous–Paleogene boundary ∼66 m.y. ago (Nicholson et al., 2022).

Here, we report on a newly discovered complex impact structure, called the Jake Seller Draw impact structure (lat 44.11°N, long 108.62°W), in the Bighorn Basin of northwestern Wyoming, western United States, which was possibly formed in a nearshore environment, with possible shallow-marine conditions. The structure is located at the northern end of the Jake Seller Draw drainage basin, leading to its name. With a depth of burial of 6.5 km and an apparent structural diameter of 4.3 km, it is the deepest impact structure discovered to date. The top of the structure studied here is buried by ∼150% of its diameter. That puts it far into the deeply buried crater category defined by Kenkmann (2021). There are just seven craters detected so far that fulfill this criterion. The impact origin of the feature was confirmed by documenting its structural characteristics and showing the presence of planar deformation features (PDFs) and planar fractures (PFs), which are impact-related shock effects. The structure is constrained in size by a seismic profile and three well-log profiles, situated inside and outside of the impact structure. We present the structure and petrography of the ultradeep crater and discuss a potential correlation with the Wyoming crater field (Kenkmann et al., 2018, 2022).

Sebastian Sturm https://orcid.org/0000-0003-3115-1445
†Sebastian.Sturm@geologie.uni-freiburg.de

GSA Bulletin;
published online 21 February 2024

https://doi.org/10.1130/B37164.1.

2. GEOLOGY OF THE BIGHORN BASIN

The Bighorn Basin of southern Montana and northwestern Wyoming is a large (~25,600 km^2) sedimentary basin, the basin axis of which trends NW-SE. It is structurally limited by the Pryor Mountains in the northeast, the Bighorn Mountains in the east, the Owl Creek uplift in the south, the Absaroka Range in the west, and Beartooth Mountains in the northwest (Figs. 1 and 2; Finn et al., 2010). The basin formed in a series of tectonic events that controlled its subsidence history, beginning with the Neoproterozoic rifting of Rodinia and the formation of the Cordilleran passive margin. Subsequent tectonic events, including the Late Devonian–early Mississippian Antler orogeny, the Pennsylvanian–Permian Ancestral Rockies orogeny, the

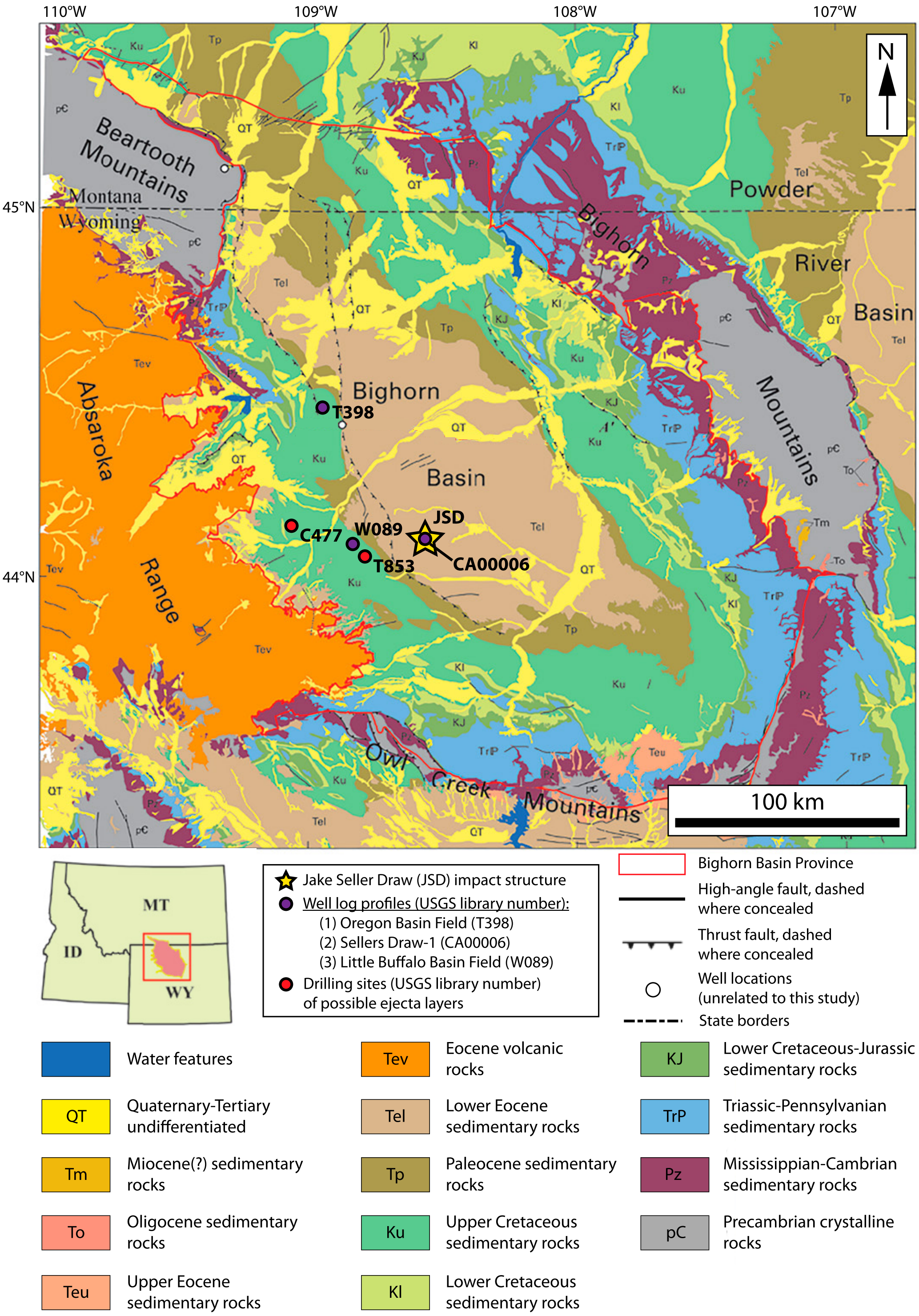

Figure 1. Geological map of the Bighorn Basin, Wyoming and Montana, modified from Finn et al. (2010). ID—Idaho; MT—Montana; WY—Wyoming.

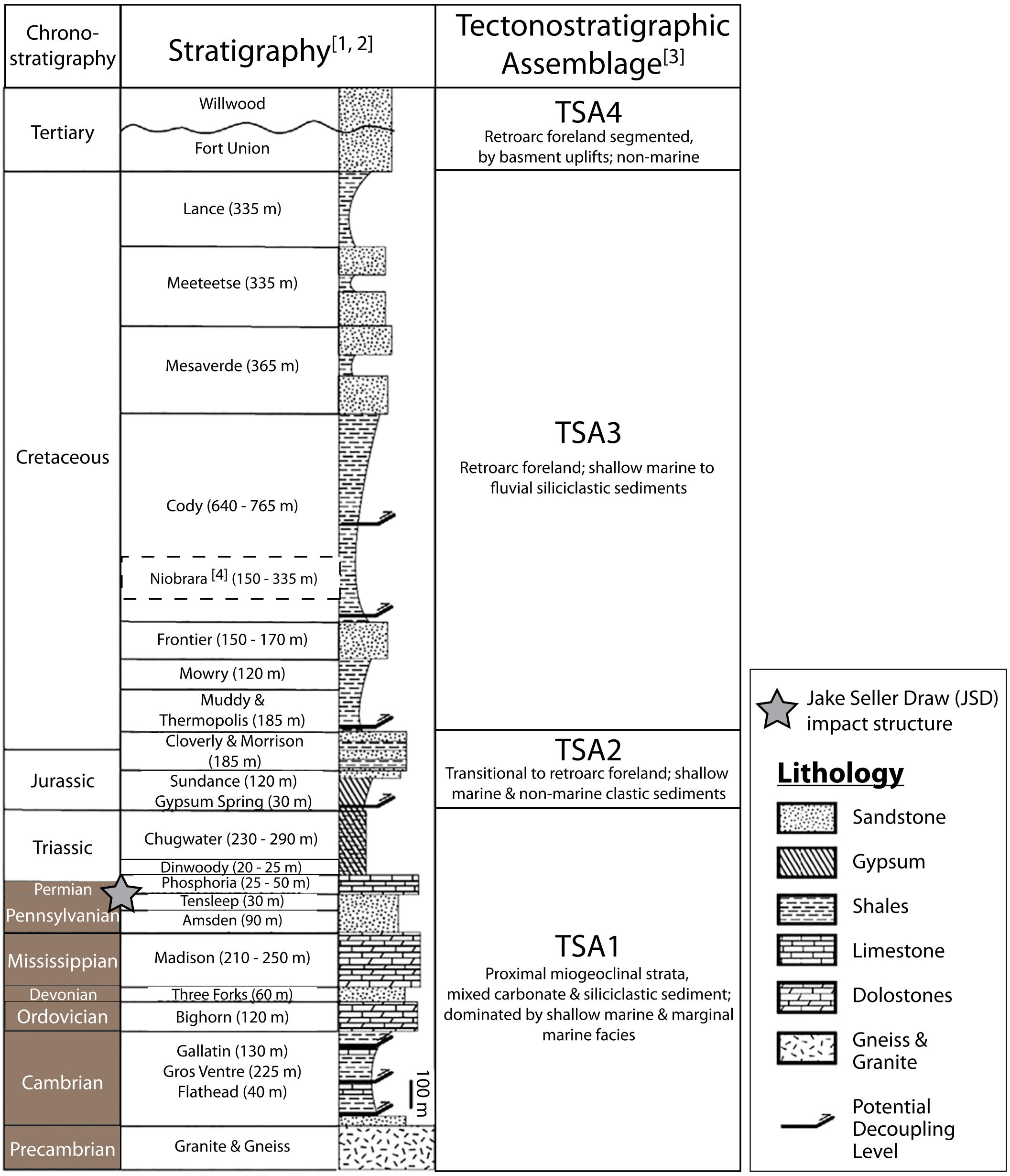

Figure 2. Synthetic stratigraphic column of the western Bighorn Basin, modified after [1] Durdella (2001), [2] Neely and Erslev (2009), [3] May et al. (2013), and [4] Finn (2019) for Niobrara interval of the Upper Cretaceous Cody Shale.

Cretaceous Sevier orogeny, and the Late Cretaceous–Paleogene Laramide orogeny, shaped the general structure of the basin (Dickinson, 2004; DeCelles, 2004; May et al., 2013). The present-day asymmetric structure of the Bighorn Basin was largely governed by the Late Cretaceous to Eocene Laramide orogeny (Figs. 1 and 2; Gries, 1983; Dickinson et al., 1988; Love, 1988). Laramide-type orogenesis is characterized by Precambrian basement-cored uplifts along steep reverse and wrench faults (e.g., Pryor, Bighorn, and Owl Creek Mountains) and intervening sedimentary basins developed over a wide area east of ~112°W longitude (Figs. 1 and 2; Coney, 1976; Dickinson et al., 1988). The uplifts are flanked by strongly folded and faulted Cambrian to Paleocene sedimentary rocks, whereas the surface of the central part of the basin is flat-lying Lower Eocene and undifferentiated Tertiary and Quaternary rocks (Figs. 1 and 2; Finn et al., 2010). The Bighorn Basin itself is filled with up to 7000 m of sedimentary rocks, which range from Cambrian to Miocene in age (Fig. 2; Pierce, 1966; Pierce and Nelson, 1968; DeCelles et al., 1991; Neely and Erslev, 2009). May et al. (2013) subdivided the Bighorn Basin into four tectonostratigraphic assemblages (TSA1–TSA4), which were determined from detrital zircon analysis (Fig. 2). The investigated Jake Seller Draw disturbance was formed in tectonostratigraphic assemblage TSA1, which is characterized by mixed carbonate and siliciclastic sediments that are dominated by shallow-marine and marginal-marine facies (Fig. 2). This interval comprises the Precambrian basement complex up to the Permian Phosphoria Formation (Fig. 2) and subsequent Triassic strata. The Precambrian basement complex (Archean crystalline basement, granites, and gneisses) is overlain by the Cambrian Flathead Formation (sandstones, ~40 m), the Gros Ventre Formation, and the Gallatin Formation (both incompetent green shales with thin interbedded limestones, ~225 m and ~130 m, respectively; Fig. 2). These Cambrian units are covered by massive, cliff-forming carbonates, which are divided into (1) the Bighorn Dolomite (Ordovician dolomites, ~120 m), (2) Jefferson/Three Forks Formation (Devonian limestones, ~60 m), and (3) Madison Limestone (Mississippian limestones, ~210–250 m; Fig. 2). These sequences are covered by the Amsden Formation (siltstones, 90 m) and the Tensleep Formation (sandstones, ~30 m; time-equivalent to the Casper Formation in southern Wyoming), followed by the Permian Phosphoria Formation (marine carbonates and black shales, ~25–50 m) or its time-equivalent red bed facies, called the Goose Egg Formation in southern Wyoming (Fig. 2). Thickness changes in the Phosphoria and Tensleep Formations are more or less compensatory, because sandstone buildups in the Tensleep Formation, usually described as dunes or "buried hills," were preserved under basal Permian sediments (Lawson and Smith, 1966; Stone, 1967; Curry, 1984; Moore, 1984).

The Absaroka Range lies at the western margin of the Bighorn Basin, and it predominantly consists of Eocene andesitic volcanic and volcaniclastic rocks that unconformably overlie folded and faulted Paleozoic, Mesozoic, and Lower Tertiary sedimentary rocks (Fig. 1; Sundell, 1990, 1993). The axis of the basin generally trends NW-SE but locally shows a N-S direction. Major thrust faults in the Bighorn Basin are the Beartooth fault, the Line Creek fault, and the Oregon Basin fault on the west side of the basin, the Elk Basin fault in the north-central part, and the Rio thrust fault on the east (Finn et al., 2010).

3. DATA AND METHODS

3.1. Samples and Drill Cores

For our study, we investigated 56 samples from three drilled wells (for locations, see Fig. 1), including (1) 49 cutting samples from the American Quasar Sellers Draw-1 well (U.S. Geological Survey [USGS] library number: CA00006; lat 44.11°N, long 108.62°W), (2) two solid core samples from the Husky Oil 87 Pitchfork well (USGS library number: C477; lat 44.15°N, long 109.06°W), and (3) five solid core samples from the Amoco 229 Little Buffalo Basin well (USGS library number: T853; lat 44.05°N, long 108.80°W). All of our studied core samples from the three drilling sites were provided by the USGS Core Research Center in Denver, Colorado, and were shipped to the Institute of Earth and Environmental Sciences in Freiburg, Germany, for further analysis.

(1) The American Quasar Sellers Draw-1 well (CA00006; lat 44.11°N, long 108.62°W) was drilled vertically by American Quasar Petroleum in 1974 to a total depth (TD) of −5989 m (−19,650 ft) in the Muddy Sandstone. In 1976, the well was deepened by the same company to a TD of −7035 m (−23,081 ft), targeting an anticlinal anomaly, which was recognized on a single two-dimensional (2-D) seismic line. The well was completed as a gas well in the Cretaceous Muddy Sandstone in 1977. It produced 96 million cubic meters (MCM) of gas through 1997. We used the depths and lithological references of the cuttings that were recorded by American Quasar and reported to the USGS Core Research Center in Denver. The original depth data were measured in feet, and the samples were identified, for example, as "SD21900" for the depth sample of chips from 21,900 ft to 21,910 ft depth. We used the original sample identifiers, but key depths are also given in meters in the text and on all figures.

(2) The Husky Oil 87 Pitchfork well (C477; lat 44.15°N, long 109.06°W) is situated ~35 km west of the center of Jake Seller Draw (Fig. 1). It was drilled by the operator Husky Oil to a TD of −1333 m (−4374 ft) in 1985. The drill site was designed to investigate a possible petroleum reservoir. The two studied core samples were obtained from the solid slabbed core, which is stored at the USGS Core Research Center in Denver. The geological context of the stratigraphic units for this drill core was taken from the USGS Well Catalog, which is available online (https://my.usgs.gov/crcwc/).

(3) The Little Buffalo Basin well (T853; lat 44.05°N, long 108.80°W) is situated in the Little Buffalo Basin, ~12.9 km W-SE of the center of Jake Seller Draw (Fig. 1). It was drilled by the operator AMOCO to a TD of −1524 m (−4999 ft) in 1981. The drill site was designed to investigate a possible petroleum reservoir. The five studied core samples were obtained from the solid slabbed core, which is stored at the USGS Core Research Center in Denver. The geological context of the stratigraphic units for this drill core was taken from the USGS Well Catalog.

3.1.1. Sample Preparation and Analysis

The cutting fragment sizes for the Sellers Draw-1 well samples ranged from 1 mm to 5 mm. We placed ~100 fragments from each of the 49 samples on glass slides and fixed them with epoxy resin. Next, we prepared standard polished thin sections of all 56 samples from all three drill cores, mentioned above, to investigate the petrography of the stratigraphy of the Jake Seller Draw structure and to search for impact-related shock effects (Goltrant et al., 1991, 1992; Stöffler and Langenhorst, 1994). We used a Leica optical microscope and a five-axis Leitz universal stage at the Institute of Earth and Environmental Sciences in Freiburg, Germany. We determined the crystallographic orientation of PDFs and PFs within quartz grains (Ferrière et al., 2009) using Stereo32 (version 1.0.1) software (Röller and Trepmann, 2008), combined with a new stereographic projection template (NSPT), which is based on the standard stereographic projection of quartz with the *c* axis plotted in the center (Ferrière et al., 2009), to index the measured crystallographic orientations of the PDFs and PFs. For all of the grains, it was only possible to index the plane based on the angle from the *c* axis, and the orientation relative to the *a* axis was not determined.

We determined the lithology of the fragments in each zone of the Sellers Draw-1 cuttings and calculated percentages of each lithology along the depth profile of the well. In the drill cores C477 and T853, both drilled at distances from Jake Seller Draw, we searched for distinct diamictite horizons near the base of the Phosphoria Formation and top of the Tensleep Formation, which are stratigraphically coincident with the Jake Seller Draw structure. These horizons would be possible ejecta deposits.

3.2. Geophysical Dataset

We used 2-D and three-dimensional (3-D) seismic images (Fig. 3) and three well-log profiles (Fig. 4), which are described in detail in the following subsections.

3.2.1. 2-D and 3-D Seismic Survey

There is a major seismic anomaly at Jake Seller Draw. It was originally recognized on a single 2-D seismic line as a possible N-S–trending anticlinal closure far below a Cretaceous Muddy Sandstone gas prospect located in the deepest section of the Bighorn Basin. The Muddy Sandstone is the top member of the formation identified as Thermopolis on Figure 2. In 2001, the ownership of the petroleum claim was transferred to the Bill Barrett Corporation. In 2006, they acquired a 106 km^2 (41 mi^2) 3-D seismic survey over the Jake Seller Draw structure. That 3-D seismic survey was acquired by Veritas DGC and processed by Tricon Geophysics, Inc., using prestack time migration (PSTM) to help image conflicting dips with different stacking velocities (Fig. 3). Acquisition parameters for the 3-D seismic survey are given in Table 1. Oil production from the Mesaverde Formation was plugged in 2013, and ownership of the well and 3-D seismic survey was ultimately transferred to Civitas Resources. The 3-D seismic survey is proprietary. Bill Barrett Corporation geoscientists Terry Barrett, Ken Parrott, and Mike Hendricks recognized a probable impact crater structure in it in late 2006, when the 3-D seismic survey processing was completed. Only a vertical time section and time slice, which were selected by Bill Barrett Corporation geoscientists to best represent the well penetration in the anticlinal anomaly, are included herein (Fig. 3). These selected seismic images were made avail-

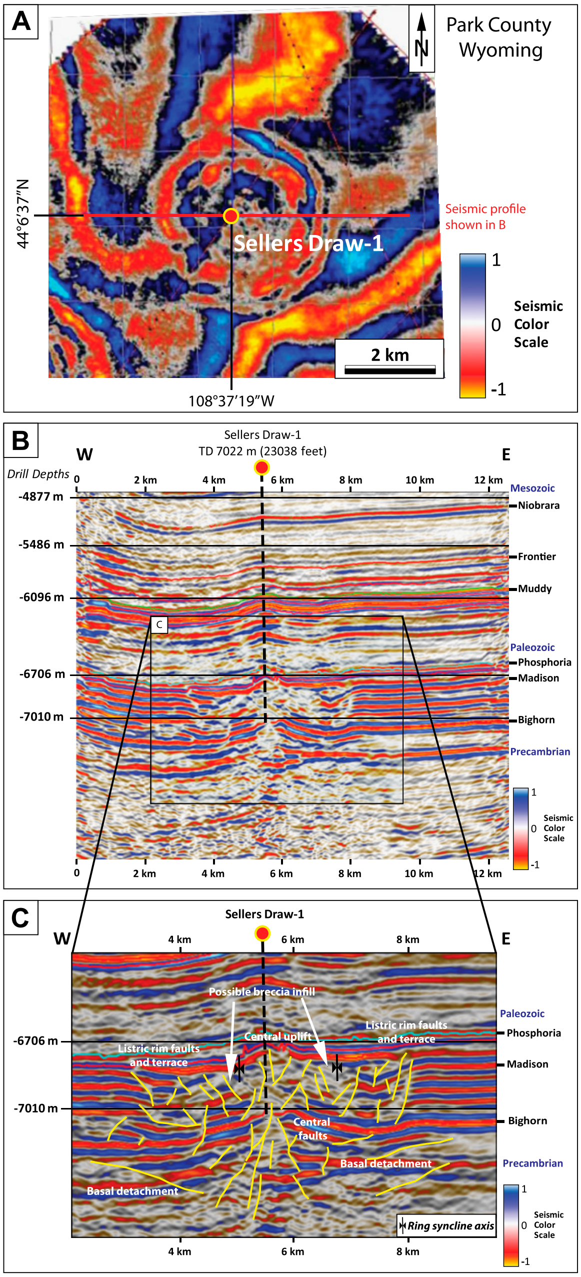

Figure 3. Three-dimensional (3-D) seismic data of Sellers Draw-1: (A) downward view showing circular structure, the orientations of sections B and C, and the location of the drill hole; (B) uninterpreted horizontal section; and (C) interpreted horizontal section. Interpreted faulting and fracturing details within the crater structure are in yellow. TD—total depth.

able to the authors with permission from Civitas Resources.

The data were provided in conventional seismic red-white-blue color scale with blue for positive amplitude, red for negative amplitude, and white representing zero (Fig. 3). The seismic amplitude scale is forced to cover a unit range in each depth zone by automatic gain control in the signal processing. We used the seismic data as a tool for structural interpretation of the Jake Seller Draw structure and made no inferences from seismic amplitude or other seismic attributes. We obtained the depth references from the Sellers Draw-1 well location, which gave us the depth of the Phosphoria Formation starting at −6594 m (−21,634 ft; top) with its base at −6654 m (−21,830 ft; Fig. 3). The vertical seismic profile that was provided for our study has ~15 times vertically exaggeration.

3.2.2. Well-Log Profiles

The stratigraphic section shown in Figure 4 presents three wells: Oregon Basin Field (USGS library number: T398; lat 44.42°N, long 108.91°W) with a TD of −1835 m, Sellers Draw-1 (USGS library number: CA00006; lat 44.11°N, long 108.62°W) with a TD of −7035 m, and Little Buffalo Basin Field (USGS library number: W089; lat 44.07°N, long 108.81°W) with a TD of −2400 m. The Sellers Draw-1 well CA00006 penetrates directly into the Jake Seller Draw seismic anomaly. The wells T398 in the Oregon Basin Field and W089 in the Little Buffalo Basin Field are situated 42 km northwest and 15 km west of Jake Seller Draw, respectively. They are upthrown and fault separated from Jake Seller Draw by the Oregon Basin thrust fault. For all three well logs (Fig. 4), the spontaneous potential (SP), gamma ray (GR), sonic (DT), and resistivity (laterolog-7 [LL7], laterolog deep [LLD], induction laterolog deep [ILD], and resistivity laterolog deep [RILD]) data are presented with stratigraphic interpretation by the Bill Barrett Corporation. On the basis of this interpreted stratigraphy, the cutting samples from Sellers Draw-1 well CA00006 from the base Phosphoria Formation (−6655 m) to TD (−7035 m) were related to possible mixed Paleozoic lithologies. These cuttings allowed us to investigate the Jake Seller Draw seismic disturbance as a possible impact structure through detailed petrographic study.

4. RESULTS

4.1. Correlated Seismic and Well-Log Data

Figure 3 shows the seismic reflection structure of Jake Seller Draw in plane view (Fig. 3A) as well as along an E-W profile (Figs. 3B and 3C). Note that the strata above the Niobrara Formation are not displayed in Figure 3B. The visible structure in Figure 3A is almost circular with an apparent diameter of 4.3 km. The borehole for Sellers Draw-1 was drilled directly into the center of the structure to a TD of −7035 m. Jake Sellers Draw seismic data show a distinct disturbance of the clearly traceable strata that are outside the structure, where strata dip very gently to the west owing to the asymmetry of the Bighorn Basin (Figs. 1 and 3B).

The continuous reflectors outside the structural disturbance can be correlated to the local stratigraphy by direct comparison with well logs from the Oregon Basin Field (T398) and the Little Buffalo Field (W089) wells, as shown in Figure 4. The Permian Phosphoria Formation is a key marker for the interpretation of the three well logs. Above the Phosphoria Formation, all three wells (Fig. 4) show tops of the Chugwater and Dinwoody Formations. All three well logs show that the Phosphoria Formation is overlain by the Dinwoody Formation, but the lower contact of the Phosphoria Formation, normally at the top of the Tensleep Formation, is significantly different at Sellers Draw-1 (CA00006). There are nine identifiable Paleozoic formations expected below the top of the Tensleep Formation. They are missing at CA00006 (Fig. 4), which passes

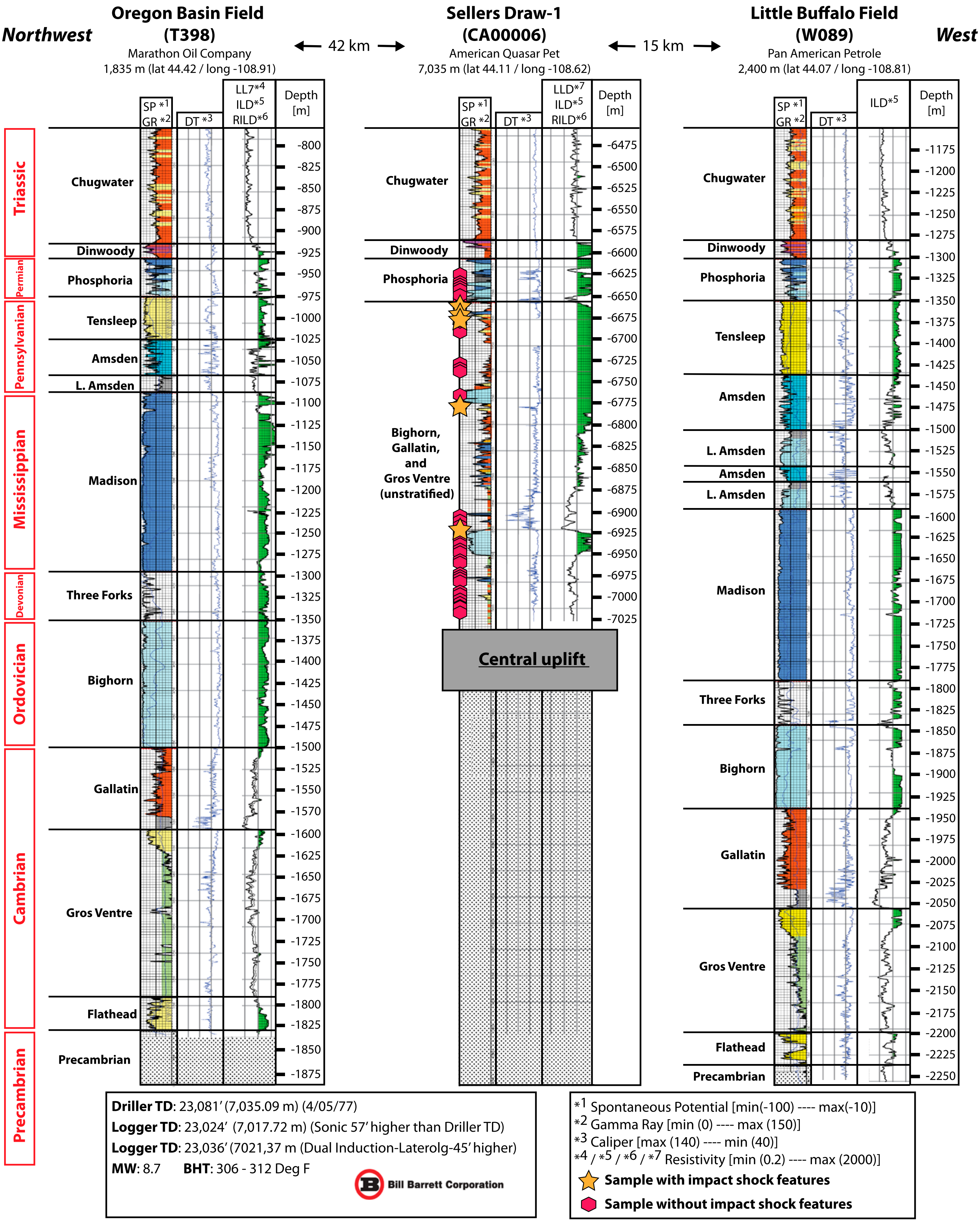

Northwest
Oregon Basin Field
(T398)
Marathon Oil Company
1,835 m (lat 44.42 / long -108.91)
42 km
Sellers Draw-1
(CA00006)
American Quasar Pet
7,035 m (lat 44.11 / long -108.62)
15 km
Little Buffalo Field
(W089)
Pan American Petrole
2,400 m (lat 44.07 / long -108.81)
West
SP *1
GR *2
DT *3
LL7*4
ILD*5
RILD*6
LLD*7
Depth [m]
Triassic
Permian
Pennsylvanian
Mississippian
Devonian
Ordovician
Cambrian
Precambrian
Chugwater
Dinwoody
Phosphoria
Tensleep
Amsden
L. Amsden
Madison
Three Forks
Bighorn
Gallatin
Gros Ventre
Flathead
Precambrian
Bighorn, Gallatin, and Gros Ventre (unstratified)
Central uplift
Driller TD: 23,081′ (7,035.09 m) (4/05/77)
Logger TD: 23,024′ (7,017.72 m) (Sonic 57′ higher than Driller TD)
Logger TD: 23,036′ (7021,37 m (Dual Induction-Laterolg-45′ higher)
MW: 8.7 BHT: 306 - 312 Deg F
Bill Barrett Corporation
*1 Spontaneous Potential [min(-100) ---- max(-10)]
*2 Gamma Ray [min (0) ---- max (150)]
*3 Caliper [max (140) ---- min (40)]
*4 / *5 / *6 / *7 Resistivity [min (0.2) ---- max (2000)]
Sample with impact shock features
Sample without impact shock features

Figure 4. Well-log stratigraphic section of the Oregon Basin Field (left), Sellers Draw-1 (middle), and Little Buffalo Basin Field (right) boreholes (see Fig. 1 for locations). Note that the Tensleep sandstone and the formations below are missing at the Sellers Draw-1 well. The seismic disturbance is at the Phosphoria-Tensleep contact. Color-coding of spontaneous potential (SP) and gamma ray (GR) logs by stratigraphy plus lithology (sand, shale, limestone) was done by the Bill Barrett Corporation in 2007. The formation identifications are from the original well logs. The chips at CA00006 below the Phosphoria Formation did not show the usual lithologies of Tensleep through Three Forks Formations. They were a match to mixed lithologies expected from the Bighorn through the Gros Ventre Formations. DT—caliper; LL7—laterolog-7; ILD—induction laterolog deep; RILD—resistivity induction laterolog deep; LLD—laterolog deep; TD—total depth; MW—megawatt; BHT—bottomhole temperature.

through the center of the circular seismic anomaly (Fig. 3). Figure 4 shows that wells T398 and W089 have the usual Tensleep through Flathead progression of Paleozoic formations below the their Phosphoria-Tensleep boundaries (Fig. 4). Well CA00006, in contrast, does not show any of these formations in the 382 m from the bottom of the Phosphoria Formation to the bottom of the well. The Phosphoria Formation at Sellers Draw-1 is ~49 m thick. It is slightly thinner at ~45 m at both the Oregon Basin and Little Buffalo Basin Fields.

The E-W profile of the Jake Seller Draw structure shown in Figures 3B and 3C reveals the complex nature of the seismic anomaly compared to the surrounding strata. There are inward-dipping listric normal faults at its edges (Fig. 3C), where the western rim fault dips ~20° less steeply than the eastern one. Beneath the rim faults at the base of the Jake Seller Draw disturbance, there are low-angle faults, which can be identified as basal detachment faults, on both sides. The upper section of the central part lacks clear seismic reflectors, compared to the more or less intact layering of the strata visible west and east outside of the seismic disturbance (Fig. 3C). In the central portion of the seismic anomaly, numerous reverse faults are visible. East and west of the central parts, there are complex synclines, each ~1200–1500 m wide, which are dissected by numerous possible smaller faults, partly with half-graben and stairstepping geometries (Fig. 3C). The whole disturbed structure itself is overlain unconformably by a continuous reflector, which is the base of the Phosphoria Formation, shown in red in Figure 3C. The trough reflector just below that increases in thickness above the synclines.

The Jake Seller Draw seismic structure is in the deepest part of the Bighorn Basin. The present-day structure of the Bighorn Basin developed substantially during the Laramide orogeny from Late Cretaceous time to early Eocene time. The section above the seismic structure starts above the red horizon of the base Phosphoria Formation in Figure 3B. Notably, the Muddy Sandstone trough reflector presents the brightest seismic amplitude and is the reservoir for gas production in the Sellers Draw-1 well. Also of note is the pronounced structural high that continues along the borehole up section to the Late Cretaceous Niobrara Formation.

TABLE 1. SEISMIC SURVEY PARAMETERS FOR SELLERS DRAW-1 THREE-DIMENSIONAL SECTION

Area	106 km^2 (41 mi^2)
Channels	1512
Source	Vibroseis
Group interval	67 m (220 ft)
Source interval	67 m (220 ft)
Source line spacing	671 m (2200 ft)
Receiver line spacing	469 m (1540 ft)
Bin size	34 × 34 m (110 × 110 ft)
Data length	5 s
Sample rate	2 ms
Live bins	94,252
Nominal fold	70

4.2. Borehole Sellers Draw-1

The overall petrographic character of the Sellers Draw-1 cutting samples below the base of the Phosphoria Formation is as a mixture of different carbonate facies, which make up ~90% of the fragments in the cutting samples, and a minor (~10%) appearance of siliciclastic sediment fragments. The majority of the 56 cutting samples from the Sellers Draw-1 drill chips are dominated by rocks from shallow-marine and marginal-marine facies. All samples along the entire depth profile from −6639 m down to −7035 m of Sellers Draw-1 include fragments of anhydrites, calcareous sandstones, a variety of dolomite fragments, micritic to intramicritic mudstones and limestones, chert fragments, quartzites, and abundant microbreccia (Fig. 5). The calcareous sandstone and dolomite fragments show a high degree of oxidation at all sample depths, as indicated by the overall reddish to brownish color of the grains (Fig. 5). Based on the first occurrence of specific lithological fragments, we subdivided the depth profile from −6639 m down to −7035 m into four main sections (Figs. 6 and 7).

Section 1 (seven samples from SD-21780 to SD-21890), with a depth interval from −6639 m to −6672 m, is characterized by several biomicrites (e.g., foraminifera) and biosparite and coral fragments, which were found sporadically in section 2 and not in the deeper sections 3 and 4 (Figs. 6A and 6B).

Section 2 (seven samples from SD-21900 to SD-21970), with a depth interval from −6675 m to −6696 m, is characterized by the first occurrences of calcareous sandstone fragments including glauconitic sandstone, in addition to shaley dolomite fragments with small zoned dolomite rhombohedrons (Figs. 6C and 6D). Zoning of dolomites can indicate more than one period of crystal growth or a change in conditions during crystallization.

Section 3 (seven samples from SD-22000 to SD-22290), with a depth interval from −6706 m to −6794 m, is characterized by the first occurrence of dolomites, which show larger zoned dolomite rhombohedrons compared to section 2, dolomite-quartzite breccias, and a breccia fragment buildup composed of shaley dolomites combined with dolomites with small zoned dolomite rhombohedrons and glauconitic sandstone (Figs. 6E and 6F).

Section 4 (28 samples from SD-22700 to SD-23070), with a depth interval from −6919 m to −7035 m, shows the first occurrence of a variety of shales. In addition, we found several brecciated fragments composed of shales and calcareous sandstones with the appearance of glauconite (Figs. 6G and 6H).

4.3. Drill Cores C477 and T853

The drill cores with USGS library numbers C477 and T853 are from wells that were located at distances of 35 km west and 12.9 km W-SE of the Sellers Draw-1 well, respectively (Fig. 1). They are well outside the seismic disturbance at Jake Seller Draw. The stratigraphic units for both drill cores were obtained from the USGS Well Catalog.

Both cores show diamictite layers (Figs. 8A and 8B). In drill core C477, we identified two diamictite horizons with thicknesses of ~8 cm and ~5 cm within the depth interval 1262–1262 m (Fig. 8A). The two horizons lie stratigraphically between the overlying Phosphoria Formation (Permian) and the underlying Tensleep Formation (Pennsylvanian). The overall lithological character of the C477 diamictite layer is a calcareous sandstone breccia, including limestone and chert fragments. Macroscopically, it shows angular limestone fragments

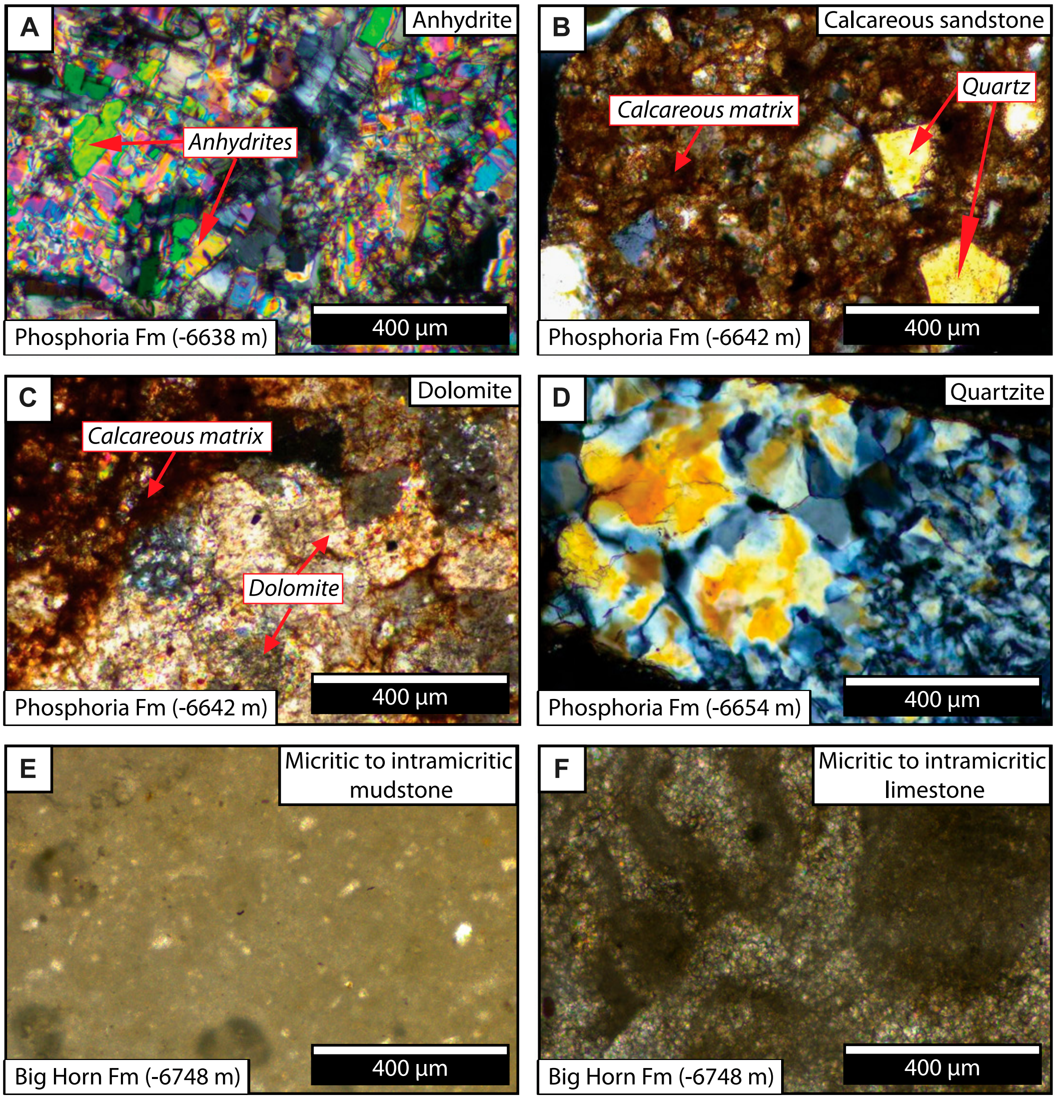

Figure 5. Main facies types in the Sellers Draw-1 drilling chips (crossed polarizers): (A) anhydrites, (B) calcareous sandstones (different stages of oxidation), (C) dolomites, (D) quartzite, (E) micritic to intramicritic mudstone, and (F) micritic to intramicritic limestone.

smaller than 5 cm in a more fine-grained calcareous sandstone matrix (Figs. 8C and 8D). The angular limestone fragments also show internal fractures (Fig. 8D). The identified diamictite layers show clear lithological differences from the overlying lighter and dense limestone of the Phosphoria Formation to the underlying darker and more fine-grained sandstone of the Tensleep Formation (Fig. 8B).

The diamictite layer identified in T853 was found stratigraphically between the overlying Phosphoria Formation and the underlying Tensleep Formation in the depth interval of 1434 m to 1435 m, and it has a thickness of ~90 cm (Fig. 8B). Similar to C477, the overall lithological character of this diamictite layer in T853 is a calcareous sandstone breccia, including limestone and chert fragments (Figs. 8E and 8F). The identified diamictite layer shows clear lithological differences from the darker and more fine-grained layers of the overlying Phosphoria Formation to the underlying Tensleep Formation (Fig. 8B). The brecciated diamictite layer of T853 shows similar angular limestone fragments, smaller than 5 cm in size, which are cemented in a fine-grained limestone to calcareous sandstone matrix (Fig. 8F).

4.4. Shock Metamorphic Microstructures

The vast majority of the quartz grains from the cutting samples of Sellers Draw-1 (USGS library number: CA00006) did not exhibit shock features. We did not find any impact-related shock features in section 1. We did, however, find seven grains from sections 2, 3, and 4 from the Sellers Draw-1 drill cuttings that exhibited PDFs, providing distinctive evidence of impact shock, and in addition, several PFs. In particular, five grains from sections 2, 3, and 4 showed multiple sets of decorated PDFs (Table 2; Fig. 9): (1) one quartz grain in a micrite fragment from SD-21900 in section 2 showed two sets of decorated PDFs parallel to $\{11\bar{2}0\}$ and subordinate $\{11\bar{2}1\}$ lamellae, (2) one quartz grain in a limestone fragment from SD-21940 in section 2 showed one set of decorated PDFs parallel to $\{10\bar{1}4\}$ lamellae, (3) one quartz grain in a marly limestone fragment from SD-21950 in section 2 showed two sets of decorated PDFs parallel to $\{10\bar{1}3\}$ and subordinate $\{01\bar{1}3\}$ lamellae, and finally, (4) two shocked quartz grains in a dolomite fragment from SD-22280 from section 3 showed three sets of decorated PDFs parallel to (0001) and subordinate $\{51\bar{6}1\}$ and $\{10\bar{1}1\}$ lamellae.

In Sellers Draw-1, additionally, two grains located in sections 2 and 4 showed multiple sets of decorated PFs (Table 2; Fig. 9): (1) one quartz grain in a limestone from SD-21940 from section 2 showed two sets of decorated PFs

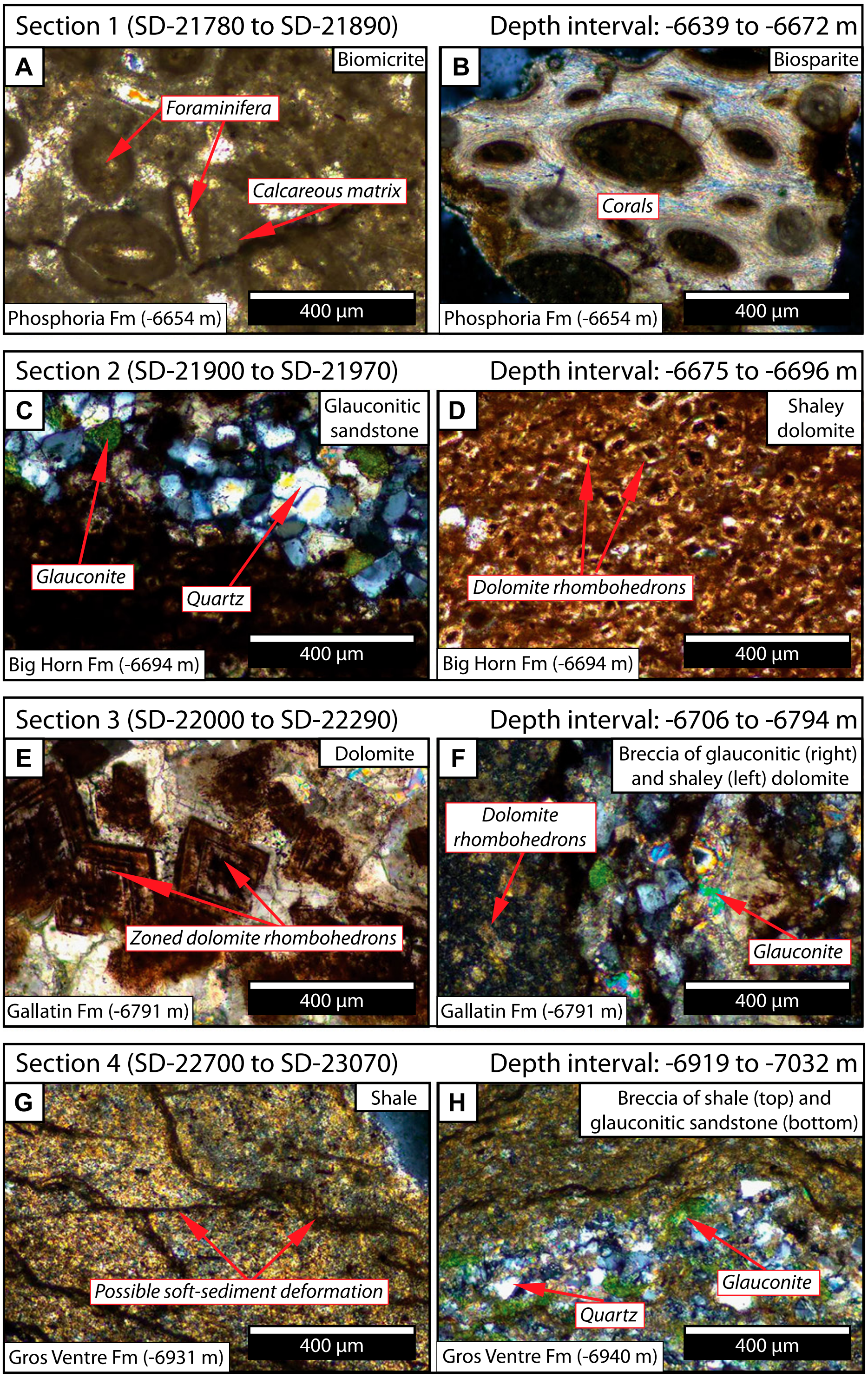

Figure 6. Specific facies types in the cutting samples from the Sellers Draw-1 drilling chips, found in the four subdivided sections of the drilling profile (crossed polarizers): Section 1 with (A) biomicrite (e.g., foraminifera) and (B) biosparite (e.g., corals), section 2 with (C) calcareous sandstone with glauconite and (D) shaley dolomite with small zoned dolomite rhombohedrons, section 3 with (E) dolomite with large zoned dolomite rhombohedrons and (F) breccia of dolomite with glauconite and shaley dolomite with small zoned rhombohedrons, and section 4 with (G) shale and (H) breccia fragment of shale and calcareous sandstone with glauconite.

parallel to $\{10\bar{1}1\}$ and subordinate to $\{04\bar{4}1\}$ lamellae, and (2) one shocked quartz grain in a calcareous sandstone fragment from SD-22750 from section 4 showed two sets of decorated PFs parallel to $\{10\bar{1}1\}$ and subordinate to $\{4\bar{2}\bar{2}1\}$ lamellae. Table 2 shows the crystallographic data for the shocked quartz samples from the Sellers Draw-1 core.

In the drill core from the Little Buffalo Basin well (T853), ~12.9 km W-SW of the center of Jake Seller Draw, we found two quartz grains from the drill core that exhibited multiple sets of decorated PDFs in a depth range of −1433.8 m to −1435 m (−4794 ft to −4708 ft; Table 2; Fig. 10): (1) one quartz grain in a calcareous sandstone from T853-4704 showed one dominant set of decorated PDFs parallel to $\{10\bar{1}3\}$ lamellae (Fig. 10A), and (2) one quartz grain in a calcareous sandstone from T853-4708 showed one set of decorated PDFs parallel to $\{10\bar{1}3\}$ lamellae (Fig. 10B).

5. DISCUSSION

5.1. Evidence for the Impact Origin of the Jake Seller Draw Structure

Several scenarios to produce large-scale (>1 km) circular crater-like structures are described in the literature, including (1) impact cratering, (2) subsurface salt withdrawal or dissolution, (3) gas or fluid escape, (4) collapsed volcanic calderas or maars, (5) collapse features associated with carbonate dissolution, (6) polygonal faulting induced by dewatering, (7) the erosive actions of currents, (8) tectonic (strike-slip pull-apart) deformation, or (9) any combination of these processes (e.g., Melosh, 1989; Stewart, 1999; Bertoni and Cartwright, 2005; McDonnell et al., 2007). Based on our findings of shock-metamorphic microstructures (PDFs and PFs) inside and outside of Jake Seller Draw, the nature of diamictite layers outside of Jake Seller Draw, structural analysis using 2-D and 3-D seismic data, and the location of the Jake Seller Draw disturbance buried in the Bighorn Basin, we discuss in the following subsections our proposed formation scenario for the Jake Seller Draw structure, formed by impact cratering, compared to the other possible formation scenarios.

5.1.1. Impact-Related Shock Effects and Deposits

The PDFs in quartz are the most important and reliable impact diagnostic criteria for meteorite impact because they cannot be formed in any other geological environment (e.g., Goltrant et al., 1991, 1992; Langenhorst and Deutsch, 1994; Stöffler and Langenhorst, 1994; Ferrière

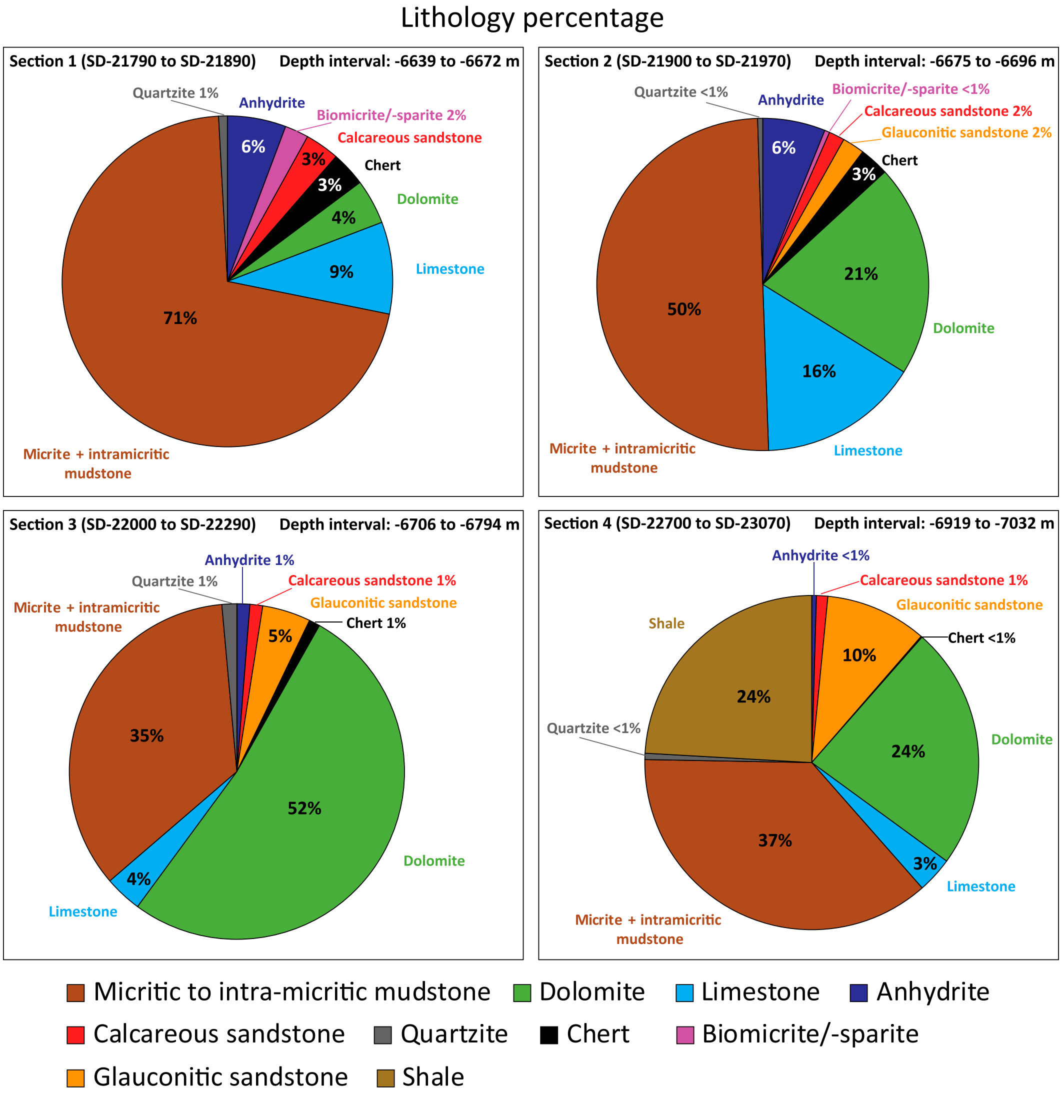

Figure 7. Pie plots of the lithology percentages in the cutting samples for each section from the Sellers Draw-1 borehole. The percentages were determined by counting chips in mountings.

et al., 2009). In total, 16 measurements in seven quartz grains from Jake Seller Draw showed lamellae orientations along (0001), {$10\bar{1}3$}, {$10\bar{1}1$}, {$11\bar{2}1$}, {$51\bar{6}1$}, {$11\bar{2}0$}, and {$10\bar{4}1$}, and subordinately along {$01\bar{1}3$}, {$04\bar{4}1$}, and {$4\bar{2}\bar{2}1$}, coinciding with the most frequent PDF and PF orientations reported in the literature (e.g., Stöffler and Langenhorst, 1994; Ferrière et al., 2009) (Table 2; Fig. 11). The relatively few shocked quartz grains in the Sellers Draw-1 cutting samples hamper statistical interpretation and shock pressure estimation. Additionally, it is unlikely to find impact-related shock features in calcite or dolomite, as they do not survive for long periods of time in the geological record. Limestone has a weak memory for a sequence of deformation phases, as calcite and dolomite recrystallize easily, even at low temperature (e.g., Langenhorst et al., 2003; Passchier and Trouw, 2005).

The cuttings are dominated by marine shale, limestone, and dolomite. The impact target Tensleep Formation is primarily sandstone, which represents only 1% of section 1, where the Tensleep Formation would be expected just below the Phosphoria Formation. We infer that the Tensleep Formation was completely excavated and ejected from the crater (Fig. 12).

Further, in the core from borehole T853, located ~12.9 km W-SW of the center of Jake Seller Draw, we discovered PDFs with {$10\bar{1}3$} orientation in two quartz grains of the diamictite samples. Due to the presence of shock effects in T853, we interpret this diamictite layer (with a thickness of ~90 cm) as an ejecta deposit, which was formed during the formation of the Jake Seller Draw impact crater (Fig. 8B).

We did not find any shock effects in the samples taken from the two diamictite layers of C477. However, these two horizons, with thicknesses of ~8 cm and ~5 cm, are breccia layers characterized by distinct lithological features (Figs. 8C and 8D) known from impact ejecta deposits of other well-known terrestrial impact craters (e.g., Bunte Breccia from the Ries crater, Germany; Hörz et al., 1983). The two separate ejecta layers could have been caused by postimpact reworking of local deposits or incorporation of local substrate during the deposition of ejecta, as was seen in the Bunte Breccia ejecta deposits of the Ries crater in Germany. The fraction of local secondary substrate that is incorporated upon collision of primary ejecta with the target surface rapidly increases with increasing distance (e.g., Hörz et al., 1983; Sturm et al., 2013).

The ejecta layers in both drill cores are stratigraphically situated between the overlying Phosphoria Formation (Permian) and the underlying Tensleep Formation (Pennsylvanian), which makes them stratigraphically equivalent with the Jake Seller Draw impact structure itself. Therefore, these ejecta layers would be consistent with a preserved ejecta blanket surrounding Jake Seller Draw (Table 2; Figs. 9 and 11).

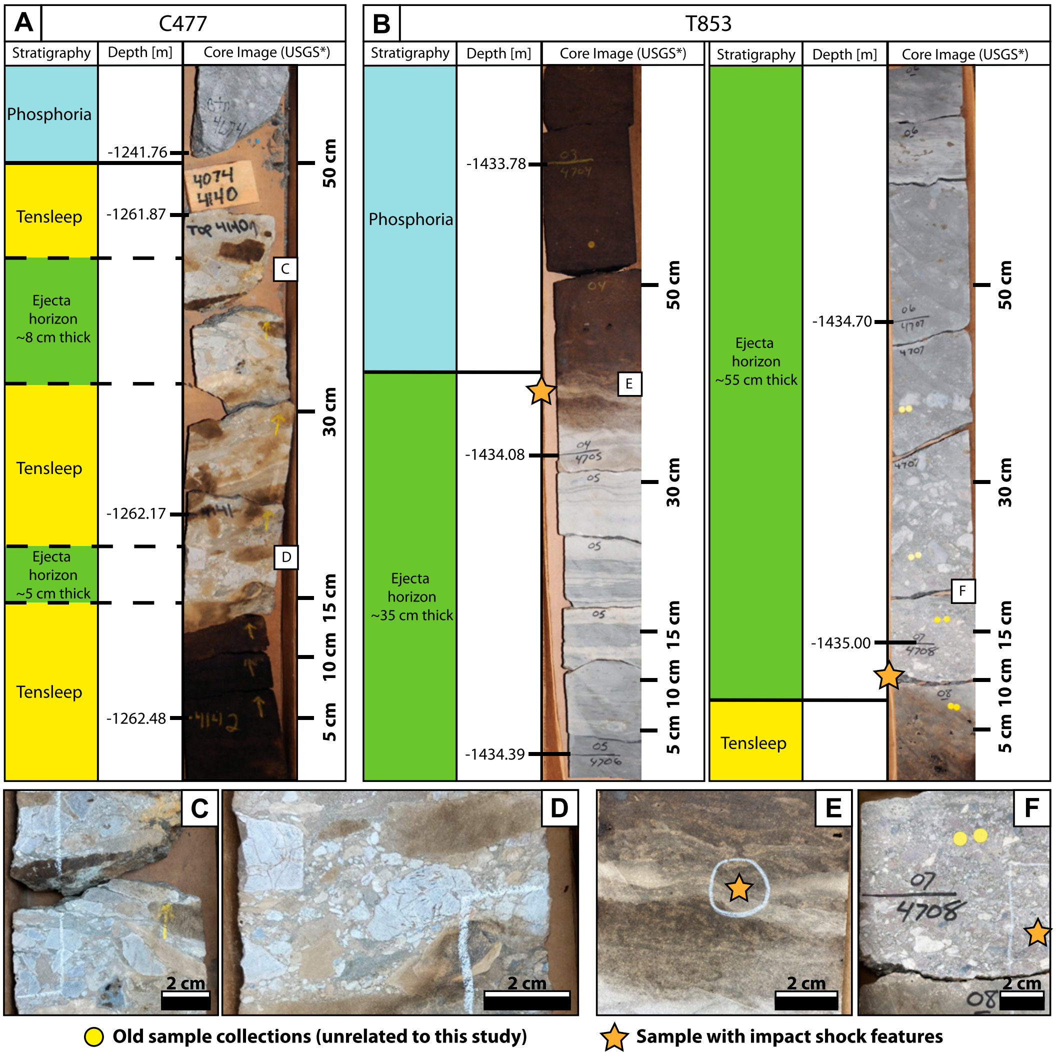

Figure 8. Core at the Phosphoria-Tensleep Formation boundary showing breccia from wells outside of studied anomalous structure: (A) U.S. Geological Survey (USGS) C477 with two breccia horizons of ~5 cm and ~8 cm thickness, at about −1262 m, and (B) USGS T853 with ~90 cm of breccia thickness between −1434 m and −1435 m depth (see Fig. 1 for locations). Both drill cores show sequences of reworked brecciated ejecta material with angular limestone clasts embedded in a limestone and calcareous sandstone matrix. (C and D) Angular limestone fragments smaller than 5 cm in a more fine-grained calcareous sandstone matrix in the two thin ejecta horizons of C477. These angular limestone fragments also show internal fractures. (E and F) Sample locations within the ejecta horizon of T853 with impact shock effects shown in Figure 10. The ejecta horizon, visible as a lighter limestone sequence, between the Phosphoria and Tensleep Formation shows in angular limestone clasts smaller than 2 cm embedded in a more fine-grained limestone matrix at the base of the ejecta horizon, as seen in part F.

The ejecta thicknesses in drill core T853, 12.9 km away from the crater center, and C477, 35 km away from the crater center, were estimated to be ~90 cm and ~5 cm to ~8 cm, respectively (Figs. 8A and 8B). These observations are similar to predicted ejecta thicknesses calculated using the Earth Impact Effects Program online to reconstruct a complex impact crater with a diameter of

TABLE 2. CRYSTALLOGRAPHIC ORIENTATIONS OF PLANAR DEFORMATION FEATURES IN SHOCKED QUARTZ FROM THE JAKE SELLER DRAW IMPACT STRUCTURE DRILL CORE (SELLERS DRAW-1*) AND FROM THE BOREHOLE CORE WITH THE U.S. GEOLOGICAL SURVEY (USGS) LIBRARY NUMBER T853 AS A POSSIBLE EJECTA LAYER OF THE JAKE SELLER DRAW IMPACT STRUCTURE†

Sample name (depth in m)	Section	Fragment lithology	Number of shocked quartz grains	Orientation of planar deformation features (PDFs) (Miller-Bravais indices {hkil})	Orientation of planar fractures (PFs) (Miller-Bravais indices {hkil})
SD-21900 (–6675)	2	Micrite	1	$\{11\bar{2}0\}$, $\{11\bar{2}1\}$	
SD-21940 (–6687)	2	Limestone	2	$\{10\bar{1}4\}$	$\{10\bar{1}1\}$, $\{04\bar{4}1\}$
SD-21950 (–6690)	2	Limestone	1	$\{10\bar{1}3\}$, $\{01\bar{1}3\}$	
SD-22280 (–6,791)	3	Dolomite	2	#1 (0001), $\{51\bar{6}1\}$, $\{10\bar{1}1\}$; #2 (0001), $\{51\bar{6}1\}$	
SD-22750 (–6934)	4	Calcareous sandstone	1		$\{10\bar{1}1\}$, $\{4\bar{2}\bar{2}1\}$
T853-4704 (–1434)	/	Calcareous sandstone	1	$\{10\bar{1}3\}$	
T853-4708 (–1435)	/	Calcareous sandstone	1	$\{10\bar{1}3\}$	

Note: For all the grains, it was only possible to index the plane based on angle from the *c* axis, and the actual orientation relative to the *a* axis is not determined.
*Nomenclature of the samples is “SD-” indicating driller’s depth in feet.
†Nomenclature of the samples is “T853” indicating depth in feet; see Figure 1 for location.

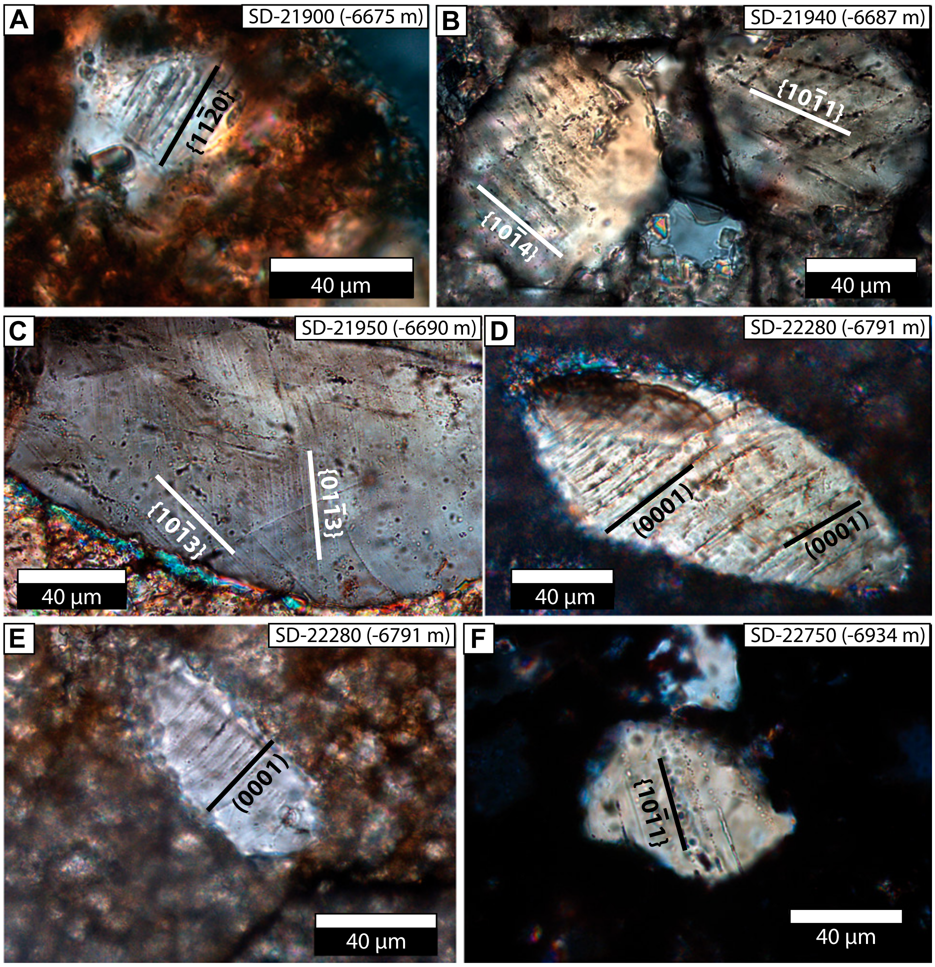

Figure 9. Shocked quartz grains investigated in the cutting samples from the Sellers Draw-1 drill core: (A) quartz grain from SD-21900 with two sets of decorated planar deformation features (PDFs) parallel to {11$\bar{2}$0} and subordinate {11$\bar{2}$1} lamellae; (B) two quartz grains from SD-21940, one (left) with a set of decorated planar deformation features parallel to {10$\bar{1}$4}, and one (right) with sets of planar fractures parallel to {10$\bar{1}$1} and one subordinate to {04$\bar{4}$1} lamellae; (C) one quartz grain from SD-21950 with two sets of decorated planar deformation features parallel to {10$\bar{1}$3} and {01$\bar{1}$3} lamellae; (D and E) two shocked quartz grains from SD-22280 with three sets of decorated planar deformation features parallel to (0001) and subordinate to {51$\bar{6}$1} and {10$\bar{1}$1} lamellae; and (F) shocked quartz grain from SD-22750 with two sets of planar fractures parallel to {10$\bar{1}$1} and subordinate to {4$\bar{2}\bar{2}$1} lamellae. All images were made under crossed polarizers.

4.3 km in a sedimentary target (https://impact.ese.ic.ac.uk/). The ejecta calculations give thicknesses of up to ~80 cm at a distance of 12.9 km from the crater center and up to ~4 cm at a distance of 35 km from the crater center.

The Sellers Draw-1 cuttings show shocked quartz and the destruction of the normal stratigraphy of the Bighorn Basin. The likely ejecta layers from outside of the structure show shocked quartz and breccia. Hence, our petrographic and microstructural analyses from inside and outside the Jake Seller Draw disturbance support its impact origin.

5.1.2. Crater Structure

The line A seismic profile provided detailed insights into the structure of the Jake Seller Draw feature (Fig. 3). The outline of the structure is defined by inward-dipping normal faults. The western rim fault dips ~20° less steeply than the eastern rim fault, which we associate with antithetic block rotations of the down-faulted units. An elevated crater rim is not preserved. A series of normal faults, partly with listric shapes, forms rotated terrace blocks that form the outer part of the ring syncline, which was also described by Kenkmann et al. (2014) for other well-known complex impact craters. Eventually, these faults merge into subhorizontal faults toward the center of the crater, as documented for other terrestrial craters by Kenkmann and von Dalwigk (2000). New structural elements, observed here for the first time, are very deeply seated detachment faults that seem to be unconnected to the normal faults (Fig. 3C). They seem to decouple the displaced crater subsurface from the unaffected basement. These detachment faults also imply a minimum depth of roughly 500 m for the seismic disturbance, measured from the contact with the overlying undeformed strata.

The central part of the crater uplifted, and the central strata moved inward and upward, which created space along the crater rim and produced the central uplift (Figs. 3, 4, and 12). Therefore, the central portion of the Jake Seller Draw structure displays uplifted strata, which are especially traceable in the lower part of the central uplift, where they appear to be more intact than at higher levels. Numerous reverse faults are visible in the centrally uplifted area (Fig. 3C).

The upper part of the central uplift lacks clear seismic reflectors, most likely due to a network of densely spaced faults and the unstratified crater infill. The lack of reflectors makes it difficult to estimate the amount of stratigraphic uplift. However, the missing strata from the Tensleep Formation down to the Three Forks Formation (Fig. 4) indicate a stratigraphic uplift of ~500 m. A pronounced structural high is visible above the central uplift of the impact crater. That uplift continues on the seismographic records up section to a location above the Late Cretaceous Niobrara Formation. This extended uplift might be indicative of structural reactivation of the crater's central uplift during Laramide compression. Measuring seismic isochron interval thicknesses, the western crater ring syncline of the Phosphoria Formation is 83% thicker than that interval outside of the crater, indicating that Phosphoria Formation sediments infilled the crater. The Muddy Sandstone to Phosphoria Formation and Frontier to Niobrara Formation intervals are isopachous across the Figure 3B seismic section. However, the Muddy to Frontier isochron interval above the crater's central uplift is only 80% as thick as it is outside of the crater. This could be indicative of a pulse of structural reactivation of the crater's central uplift during Late Cretaceous Frontier deposition ca. 90 Ma. A tectonized impact crater central peak is also observed in the Cloud Creek, Red Wing Creek, and Mjolnir impact craters (Stone and Therriault, 2003; Herber et al., 2022; Corseri et al., 2020).

East and west of the central uplift (Fig. 3), there are complex synclines, each 1200–1500 m wide, which are dissected by numerous faults, partly with half-graben and stairstepping geometries. The synclines are potentially filled with

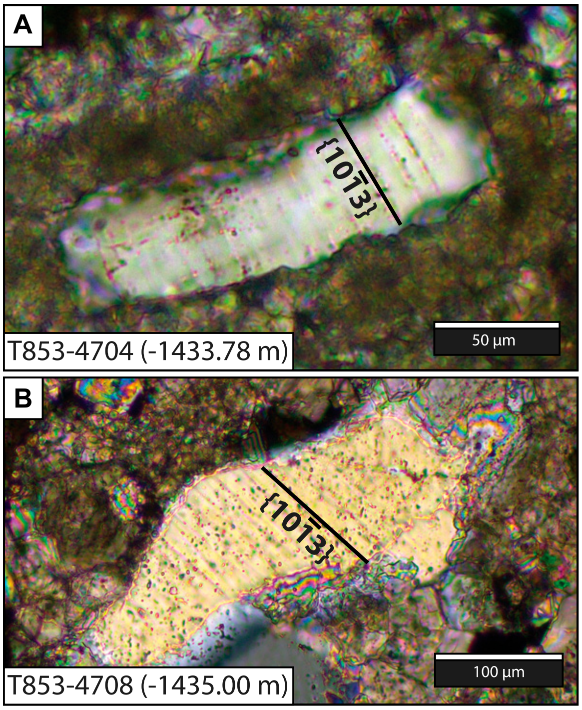

Figure 10. Shocked minerals of the ejecta samples from T853, situated outside of the Jake Sellers Draw impact structure (see Fig. 1 for location): (A) quartz grain from T853-4704 with one dominant set of decorated planar deformation features (PDFs) parallel to {10$\bar{1}$3} and (B) one quartz grain from T853-4708 with one dominant set of decorated planar deformation features parallel to {10$\bar{1}$3} lamellae.

up to 50 m of breccia, which is indicated by the absence of coherent reflectors. We identified a more or less disturbed zone above the central uplift, specifically in the area from the center of the structure out to the terraced outer zone with listric faulting. This material could represent the chaotic deposition of the possible breccia infill, with no visible layering of the original sediment stratigraphy, which was described for the lithology of the cutting samples of sections 2, 3, and 4 from the Sellers Draw-1 well (Figs. 3 and 6). The disturbed structure is overlain unconformably by a continuous reflector, which is the base of the Phosphoria Formation (red on Fig. 3). The trough reflector just below that increases in thickness above the synclines. Stratigraphic correlation suggests that the Madison Limestone and Amsden Formations and the Tensleep Formation were disturbed, while the continuous reflector above the unconformity is the base of the Phosphoria Formation (Figs. 3 and 4). The continuous basal Phosphoria reflector and the thick trough below it display a down-sagging trend above the synclines and a rise above the central uplift. In conclusion, the seismic disturbance shows all elements of a complex impact structure with a central uplift (Kenkmann et al., 2014).

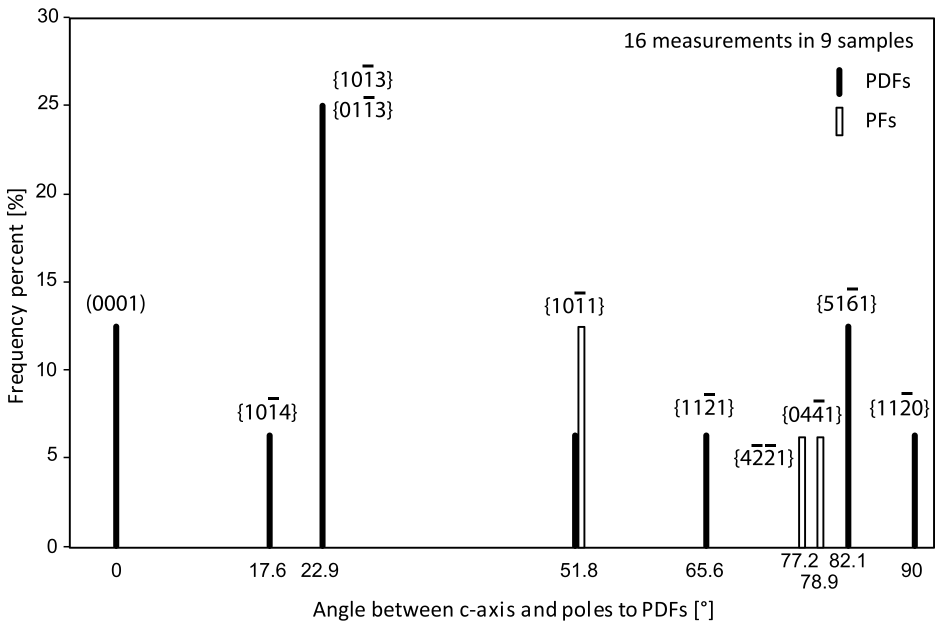

Figure 11. Crystallographic orientations of planar deformation features (PDFs) and planar fractures (PFs) in the samples inside and outside of Jake Seller Draw seismic disturbance area. The frequency of crystallographic directions of PDFs and PFs is displayed as the angle between the quartz *c* axis and the measured shock lamellae for all measurements.

5.1.3. Excavation Depth and Transient Cavity Size

Evidence of excavation can first be inferred from the missing Tensleep Formation sandstone below the Phosphoria Formation in the Seller's Draw-1 well (Figs. 4 and 12). A schematic stratigraphic section of Jake Seller Draw is shown in Figure 12, which demonstrates the relation of the three drill sites Oregon Basin Field (T398), Sellers Draw-1 (CA00006), and Little Buffalo Field (W089). It also shows the affected stratigraphic units during the formation of the Jake Seller Draw structure (Fig. 4).

The Tensleep Formation sandstone is the inferred impact target rock. As several samples from sections 2, 3, and 4 of Sellers Draw-1 drill chips show impact-related shock effects, we assume that these sections could either represent brecciated crater-fill material deposited in the center of the crater structure or material of the central uplift (Figs. 4 and 12). The overall petrographic character of the Sellers Draw-1 cutting samples below the base of the Phosphoria Formation is dominated by a mixture of carbonates. There is only a minor amount of siliciclastic sediments. The carbonates correlate with the massive Bighorn dolomites, and the lower parts correlate with the Gallatin and Gros Ventre shales, which most likely represent displaced strata from the central uplift (Figs. 2 and 12). This assumption was verified by a detailed comparison of three well-log profiles from the Oregon Basin Field, Sellers Draw-1, and Little Buffalo Basin Field wells. The profiles show that the stratigraphic sequences of the Tensleep Formation (sandstones, ~30 m), Amsden Formation (siltstones, 90 m), and Madison Formation (Mississippian limestone, ~210–250 m) down to the Three Forks Formation (Devonian limestone, ~60 m) are missing in the Sellers Draw-1 borehole profile (Fig. 4). The missing stratigraphy fits perfectly with the petrographic analyses of our cutting samples, which indicated only a minor appearance of siliciclastic sediments, as described above (Fig. 4). We did not find a sig-

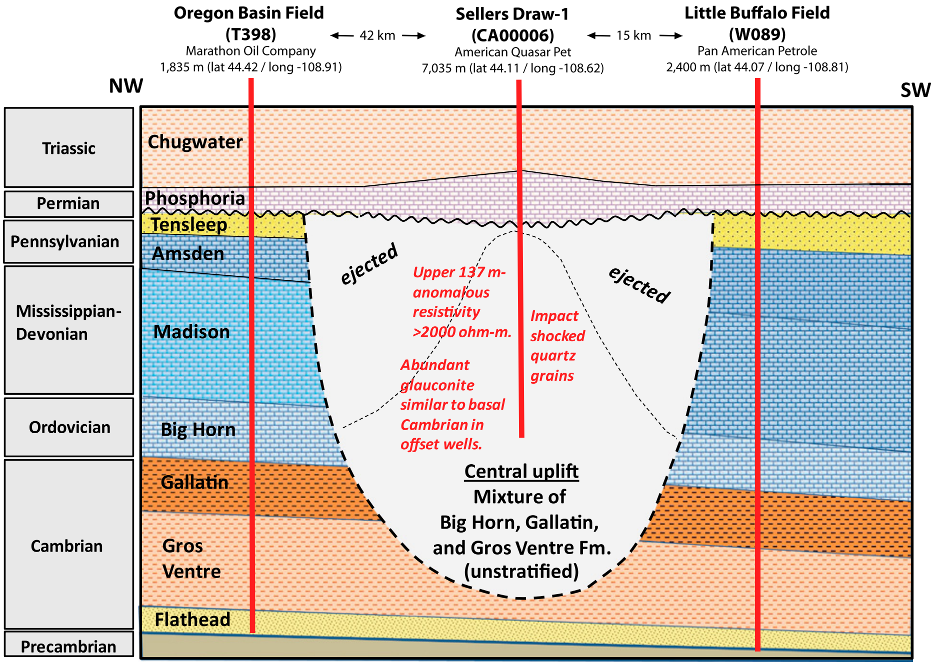

Figure 12. Schematic cross section showing the Jake Seller Draw structure in relation to the stratigraphic units that were affected by the impact formation.

nificant amount of typical Tensleep sandstones or Madison limestone fragments from sections 2, 3, and 4. Such Paleozoic fragments would generally be present in this region and depth profile of the Bighorn Basin, and we found them in the close-by Oregon Basin Field and Little Buffalo Basin Field boreholes (Fig. 4). We conclude that the complete strata sequence from the Tensleep Formation down to the Three Forks Formation, having a total thickness from ~410 m up to 540 m (Fig. 4), is missing in the Sellers Draw-1 borehole. This strata sequence was most likely excavated by the impact event. The maximum depth of crater excavation is about one-third of the transient crater depth, which, in turn, is about one-third of the transient diameter (Melosh, 1989). Taking an average of 450 m of missing strata, we infer ~1360 m and ~4100 m for the transient crater depth and crater diameter, respectively. The ejecta filled the ring syncline but are virtually absent above the central uplift, where the borehole is situated.

In addition, the more siliciclastic compositions of the ejecta layers from C477 and T853 suggest that they belong to the younger stratigraphic layers of the Tensleep Formation, which are missing in the center of the crater structure, due to their excavation during the Jake Seller Draw crater formation (Fig. 12). The Pennsylvanian–Permian Tensleep Sandstone predominantly includes fine- to medium-grained sandstone, with carbonate rocks and shale (Lawson and Smith, 1966).

5.1.4. Impact Environment and Formation Age

We did not find any impact-related shock effects in the section 1 cuttings from the Sellers Draw-1 drilling. The lithology and faunal content of section 1 match the postimpact Phosphoria Formation. The Phosphoria Formation would have been deposited into the open modified cavity of the Jake Seller Draw impact structure. These lithologic and shock observations fit our interpretation of the Sellers Draw-1 borehole, which shows the boundary between the overlying Phosphoria Formation and infill crater breccia at a depth of about −6657 m (Fig. 4). Thus, based on petrophysical well-log correlation and stratigraphy, it is possible to define the lithostratigraphic age of the Jake Seller Draw impact structure to be ca. 280 Ma, at the unconformable Pennsylvanian–Permian boundary.

From the lithology and fauna of CA00006 section 1 borehole chips, we infer that the Jake Seller Draw structure was formed in a nearshore environment, with possible shallow-marine conditions (e.g., Todd, 1964; May et al., 2013). This inference is further supported by the perfect preservation of the crater structure at depth and the preservation of impact ejecta. Ormö and Lindström (2000), Poag et al. (2004), and Kenkmann (2021) described specific characteristic features that are distinctive for craters formed in submarine conditions: (1) a nested crater morphology; (2) the replacement of a clear crater rim by a broad brim zone that may be radially dissected by resurge gullies; and (3) a thick sequence of resurge deposits within the crater depression, with indications of soft sediment deformation, and a continuous postimpact sediment sequence.

A nested crater morphology could not be detected at Jake Seller Draw. The formation of nested craters requires a significant difference between the surficial layers and the substrate in properties such as strength, density, and wave speed (e.g., Quaide and Oberbeck, 1968; Ormö, 2015). As the Precambrian basement was not affected by the formation of the Jake Seller Draw disturbance, and only sedimentary layers were involved during the impact process, a significant difference in the rheological characteristics is missing and most likely hindered the formation of a nested crater structure (Fig. 12). Nevertheless, the missing crater rim is indeed supportive for a marine impact (Figs. 3 and 4). The possible shallow-marine impact scenario at the Jake Seller Draw impact structure would have caused a forceful sediment-laden resurge into the crater. The sedimentation would eventually grade into the normal ongoing shelf sedimentation. The result would be a crater structure overburden composed of undeformed postimpact sediments of the Phosphoria Formation, which is what we observe (Figs. 3 and 4).

The Jake Seller Draw impact structure is buried at a depth of ~6.5 km in the Bighorn Basin, and hence, it is the most deeply buried known impact structure on Earth (Figs. 3 and 6), followed by the Newporte structure, which is buried 3 km (Koeberl and Reimold, 1995). The top of the structure studied here is buried by ~150% of its diameter, which puts it far into the deeply buried crater category by Kenkmann (2021). In this context, the great burial depth is attributed to sediment accommodation space created by tectonic subsidence of the Bighorn Basin (Hagen et al., 1985; Clyde et al., 2007).

Taking the impact environment into account, the Bighorn Basin is described as a huge depositional center (e.g., Hagen et al., 1985; Clyde et al., 2007), and it could be argued that the shocked quartz grains that were deposited in the Bighorn Basin originated from a distant unknown source crater. Additionally, the extensive presence of carbonates in the region and the fact that the Jake Seller Draw structure is situated in a Paleozoic nearshore environment could also lead to the assumption that the Jake Seller Draw structure represents a collapse feature associated with carbonate dissolution or was caused by erosive actions of currents. However, neither of these formation scenarios can explain the central uplift of the strata and the rotated terrace features visible in the seismic anomaly (see

Section 5.3; Fig. 3). Both phenomena were most likely caused by the formation of the Jake Seller Draw structure as a complex impact crater. Such central uplifts and rotated terraces are well documented for several complex impact craters (e.g., Kenkmann et al., 2014).

Hence, the overall combination of the complex nature of the Jake Seller Draw structure with a visible central uplift and rotated terraces, as seen in the 2-D and 3-D seismic imagery (Fig. 3), and the shocked quartz grains found in the well cutting samples from the center and outside of the Jake Seller Draw structure (Fig. 9) clearly supports the view that the Jake Seller Draw structure was formed by an impact. Therefore, the discovered shocked samples can be described as in situ shocked samples, which were generated during the formation of the Jake Seller Draw impact structure.

5.2. Relation of Jake Seller Draw Impact Structure and the Wyoming Secondary Crater Field

The Jake Seller Draw impact structure is ~300 km from the Wyoming secondary crater field (Fig. 13). Interestingly, it is also within the SE-NW alignment of secondary crater field locations and the location of the proposed possible primary crater of the crater field itself (Kenkmann et al., 2022; Fig. 13). In this context, the location of the primary crater was derived using trajectories, which were reconstructed using the orientation of the long axis of the secondary craters, when the ellipticity of a crater was larger than 1.2 and the outline of the crater was clearly defined (Kenkmann et al., 2022).

Additionally, both impact features have, within stratigraphic resolution, the same age. The impact age of the secondary crater field is inferred to be immediately after Casper Formation (Tensleep Formation time-equivalent unit in southern Wyoming) deposition and before the deposition of the Opeche Member of the Goose Egg Formation (Phosphoria Formation time-equivalent unit in southern Wyoming). This sedimentologic boundary indicates that the impact event occurred in the early Permian in the Leonardian North American Stage at ±280 Ma. No crater filling with younger Casper sandstone in the examined secondary craters was found. Only some craters have some remnant Opeche siltstone preserved in their centers. The deposition of muds started immediately after formation of craters (Kenkmann et al., 2018).

Taking these three observations into account, the geographic position of the Jake Seller Draw impact structure, the NE-SW alignment, and the same formation age, we suggest the possibility of the coincident formation of the Jake Seller Draw

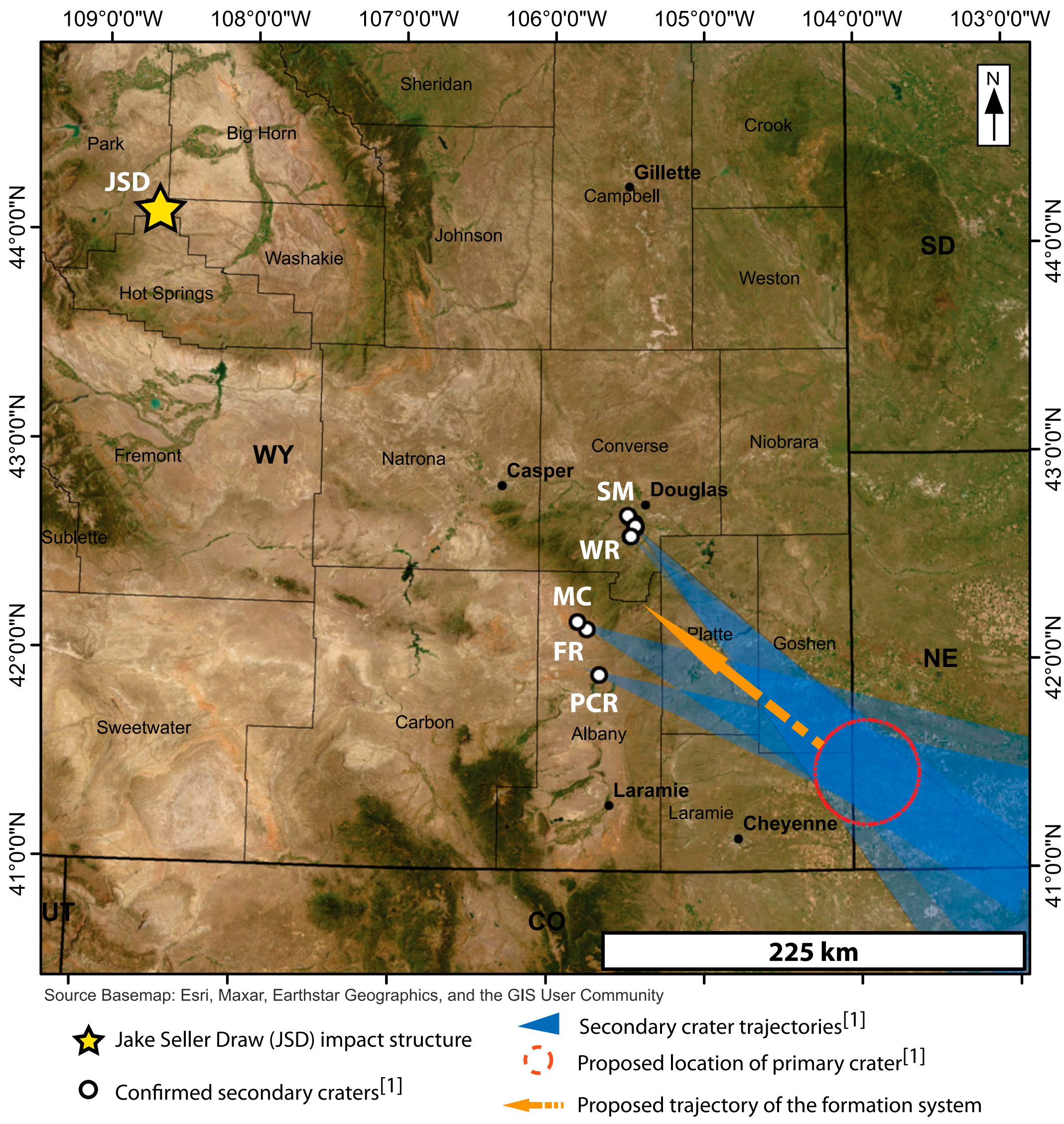

Figure 13. Map showing the geographic position of the Jake Seller Draw (JSD) impact structure in relation to the Wyoming secondary crater field (SM—Sheep Mountain; MC—Mule Creek; FR—Fetterman Ridge; PCR—Palmer Canyon Road; WR—Wagonhound Ridge) and the proposed location of the primary crater by [1] Kenkmann et al. (2022). ArcGIS base map. WY—Wyoming; SD—South Dakota; NE—Nebraska; CO—Colorado.

impact structure and the Wyoming secondary crater field. One mechanism could be a binary system comprising an asteroid that produced the Wyoming secondary crater field and its smaller moon that produced the buried Jake Seller Draw impact structure. Nevertheless, this hypothesis needs further investigation, which could include precise modeling of both proposed formation scenarios for the secondary crater field and the Jake Seller Draw impact structure, in addition to precise radiometric dating of both formations.

6. CONCLUSIONS

We documented multiple sets of PDFs in quartz grains, dominantly with (0001) and $\{11\bar{2}0\}$ orientations, and PFs, dominantly with $\{10\bar{1}1\}$ orientations, from inside the Jake Seller Draw seismic disturbance. In addition, we discovered PDFs dominantly with $\{10\bar{1}3\}$ orientations in diamictite samples of the drill core T853 outside of the crater structure in a horizon that forms the boundary between the Pennsylvanian–Permian Tensleep Formation and the Permian Phosphoria Formation. The documentation of PDFs and PFs provides proof of the impact origin of the 4.3-km-diameter Jake Seller Draw seismic disturbance. The 3-D seismic profile of the buried impact structure provides structural details that show that a complex impact structure with an $\sim$1-km-wide central uplift surrounded by a 1.2–1.5-km-wide ring syncline that comprises a system of rotated terrace blocks. The excavation depth of the crater was determined to be 400–500 m. The Jake Seller Draw impact structure is buried at a depth of $\sim$6.5 km below the surface of the Bighorn Basin and, therefore, represents the deepest buried impact structure yet discovered on Earth. The stratigraphic framework suggests that the crater was formed in a coastal or nearshore environment with shallow-marine conditions at the Pennsylvanian–Permian boundary, $\sim$280 m.y. ago. The coincident stratigraphic age of the Jake Seller Draw impact structure with the ages of the Wyoming crater field, its alignment on the same SE-NW trajectory as the proposed source crater of the Wyoming crater field, and their spatial position ($\sim$300 km distance) suggest a causal relationship between the Jake Seller Draw structure and the Wyoming crater field. The causal relationship could include the oblique collision of a binary asteroid with Earth.

ACKNOWLEDGMENTS

The authors wish to thank Paul Weimer, Paul M. Rady Endowed Chair, Department of Geological Sciences, University of Colorado–Boulder, who brought to our attention the Jake Seller Draw structure in the framework of an investigation of the Wyoming crater field. We thank geologists Terry Barrett, Ken Parrott, Mike Hendricks, and Rick Davis for their expertise, discussions, and prior impact interpretation regarding the Jake Seller Draw structure. We acknowledge and credit American Quasar Petroleum for drilling the Sellers Draw-1 well that penetrates the impact structure and recording the well data. We acknowledge and credit Bill Barrett Corporation for the 3-D seismic data that image the Jake Seller Draw buried impact structure. We acknowledge and thank Civitas Resources, the current data owner, and Terry Barrett and Bryan Richter for securing permission to publish Sellers Draw data. We acknowledge and thank the U.S. Geological Survey Core Research Center in Denver for access to cuttings and core samples from the Jake Seller Draw structure. We thank Carl Alwmark and Matthew S. Huber for their thoughtful and constructive reviews. We acknowledge the efforts of the science editor, Mihai Ducea, and the associate editor, Christian Koeberl. We thank Dagmar Flemming and Gordon Mette for the preparation of all thin sections for this project. We acknowledge continuous funding by the German Research Foundation through grant KE 732/30-1.

REFERENCES CITED

Bertoni, C., and Cartwright, J., 2005, 3D seismic analysis of circular evaporite dissolution structures, Eastern Mediterranean: Journal of the Geological Society, v. 162, no. 6, p. 909–926, https://doi.org/10.1144/0016-764904-126.

Clyde, W.C., Hamzi, W., Finarelli, J.A., Wing, S.L., Schankler, D., and Chew, A., 2007, Basin-wide magnetostratigraphic framework for the Bighorn Basin, Wyoming: Geological Society of America Bulletin, v. 119, p. 848–859, https://doi.org/10.1130/B26104.1.

Coney, P.J., 1976, Plate tectonics and the Laramide orogeny, *in* Woodward, L.A., and Northrop, A.S., eds., Tectonics and Mineral Deposits of Southwestern North America: New Mexico Geological Society Special Publication 6, p. 5–10, https://nmgs.nmt.edu/publications/special/6/home.cfm.

Corseri, R., Gac, S., Faleide, J., and Planl, S., 2020, The tectonized central peak of the Mjølnir impact crater, Barents Sea: Journal of Structural Geology, v. 131, https://doi.org/10.1016/j.jsg.2019.103953.

Curry, W.H., III, 1984, Paleotopography at the top of the Tensleep Formation, Bighorn Basin, Wyoming, *in* Morton, D., and Goolsby, J., eds., Wyoming Geological Association 36th Annual Field Conference Guidebook (1984): Casper, Wyoming, Wyoming Geological Association, p. 199–212.

DeCelles, P.G., 2004, Late Jurassic to Eocene evolution of the Cordilleran thrust belt and foreland basin system, western U.S.A.: American Journal of Science, v. 304, no. 2, p. 105–168, https://doi.org/10.2475/ajs.304.2.105.

DeCelles, P.G., Gray, M.B., Ridgway, K.D., Cole, R.B., Srivastava, P., Pequera, N., and Pivnik, D.A., 1991, Kinematic history of a foreland uplift from Paleocene synorogenic conglomerate, Beartooth Range, Wyoming and Montana: Geological Society of America Bulletin, v. 103, p. 1458–1475, https://doi.org/10.1130/0016-7606(1991)103<1458:KHOAFU>2.3.CO;2.

Dickinson, W.R., 2004, Evolution of the North American Cordillera: Annual Review of Earth and Planetary Sciences, v. 32, p. 13–45, https://doi.org/10.1146/annurev.earth.32.101802.120257.

Dickinson, W.R., Klute, M.A., Hayes, M.J., Janecke, S.U., Lundin, E.R., McKittrick, M.A., and Olivares, M.D., 1988, Paleogeographic and paleotectonic setting of Laramide sedimentary basins in the central Rocky Mountain region: Geological Society of America Bulletin, v. 100, p. 1023–1039, https://doi.org/10.1130/0016-7606(1988)100<1023:PAPSOL>2.3.CO;2.

Durdella, M.J., 2001, Mechanical Modeling of Fault-Related Folds: West Flank of the Bighorn Basin, Wyoming [M.S. thesis]: West Lafayette, Indiana, Purdue University, 128 p.

Erslev, E.A., and Koenig, N.V., 2009, Three-dimensional kinematics of Laramide, basement-involved Rocky Mountain deformation, USA: Insights from minor faults and GIS-enhanced structure maps, *in* Kay, S.M., Ramos, V.A., and Dickinson, W.R., eds., Backbone of the Americas: Shallow Subduction, Plateau Uplift, and Ridge and Terrane Collision: Geological Society of America Memoir 204, p. 125–150, https://doi.org/10.1130/2009.1204(06).

Ferrière, L., Morrow, J.R., Amgaa, T., and Koeberl, C., 2009, Systematic study of universal-stage measurements of planar deformation features in shocked quartz: Implications for statistical significance and representation of results: Meteoritics & Planetary Science, v. 44, no. 6, p. 925–940, https://doi.org/10.1111/j.1945-5100.2009.tb00778.x.

Finn, T.M., 2019, Stratigraphic Cross Sections of the Niobrara Interval of the Upper Cretaceous Cody Shale in the Bighorn Basin, Wyoming and Montana: U.S. Geological Survey Scientific Investigations Map 3422, pamphlet, 19 p. and 1 sheet [cross section], https://doi.org/10.3133/sim3422.

Finn, T.M., Kirschbaum, M.A., Roberts, S.B., Condon, S.M., Roberts, L.N.R., and Johnson, R.C., 2010, Cretaceous–Tertiary Composite Total Petroleum System (503402), Bighorn Basin, Wyoming and Montana, *in* U.S. Geological Survey Bighorn Basin Assessment Team, eds., Petroleum Systems and Geologic Assessment of Oil and Gas in the Bighorn Basin Province, Wyoming and Montana: U.S. Geological Survey Digital Data Series DDS-69-V, 156 p., https://doi.org/10.3133/ds69 V.

French, B.M., and Koeberl, C., 2010, The convincing identification of terrestrial meteorite impact structures: What works, what doesn't and why: Earth-Science Reviews, v. 98, p. 123–170, https://doi.org/10.1016/j.earscirev.2009.10.009.

Goltrant, O., Cordier, P., and Doukhan, J.-C., 1991, Planar deformation features in shocked quartz: A transmission electron microscopy investigation: Earth and Planetary Science Letters, v. 106, no. 1–4, p. 103–115, https://doi.org/10.1016/0012-821X(91)90066-Q.

Goltrant, O., Leroux, H., Doukhan, J.-C., and Cordier, P., 1992, Formation mechanisms of planar deformation features in naturally shocked quartz: Physics of the Earth and Planetary Interiors, v. 74, no. 3–4, p. 219–240, https://doi.org/10.1016/0031-9201(92)90012-K.

Gottwald, M., Kenkmann, T., and Reimold, W.U., 2020, Terrestrial Impact Structures: The TanDEM-X Atlas: Münich, Germany, Dr. Pfeil Verlag, 608 p.

Gries, R., 1983, Oil and gas prospecting beneath Precambrian of foreland thrust plates in the Rocky Mountains: American Association of Petroleum Geologists Bulletin, v. 67, no. 1, p. 1–26, https://doi.org/10.1306/03B5ACB4-16D1-11D7-8645000102C1865D.

Gulick, S.P.S., Christeson, G.L., Barton, P.J., Grieve, R.A.F., Morgan, J.V., and Urrutia-Fucugauchi, J., 2013, Geophysical characterization of the Chicxulub impact crater: Reviews of Geophysics, v. 51, no. 1, p. 31–52, https://doi.org/10.1002/rog.20007.

Hagen, E.S., Shuster, M.W., and Furlong, K.P., 1985, Tectonic loading and subsidence of intermontane basins: Wyoming foreland province: Geology, v. 13, p. 585–588, https://doi.org/10.1130/0091-7613(1985)13<585:TLASOI>2.0.CO;2.

Herber, B., Weimer, P., Bouroullec, R., Barton, R., Behringer, D., Hammon, W., III, and Gutterman, W., 2022, Three-dimensional seismic interpretation of a meteorite impact feature, Red Wing Creek field, Williston Basin, western North Dakota: American Association of Petroleum Geologists Bulletin, v. 106, no. 7, p. 1499–1546, https://doi.org/10.1306/02032217261.

Hörz, F., Ostertag, R., and Rainey, D.A., 1983, Bunte Breccia of the Ries: Continuous deposits of large impact craters: Reviews of Geophysics, v. 21, no. 8, p. 1667–1725, https://doi.org/10.1029/RG021i008p01667.

Kenkmann, T., 2021, The terrestrial impact crater record: A statistical analysis of morphologies, structures, ages, lithologies, and more: Meteoritics & Planetary Science, v. 56, no. 5, p. 1024–1070, https://doi.org/10.1111/maps.13657.

Kenkmann, T., and von Dalwigk, I., 2000, Radial transpression ridges: A new structural feature of complex impact craters: Meteoritics & Planetary Science, v. 35, no. 6, p. 1189–1201, https://doi.org/10.1111/j.1945-5100.2000.tb01508.x.

Kenkmann, T., Poelchau, M.H., and Wulf, G., 2014, Structural geology of impact craters: Journal of Structural Geology, v. 62, p. 156–182, https://doi.org/10.1016/j.jsg.2014.01.015.

Kenkmann, T., Afifi, A.M., Stewart, S.A., Poelchau, M.H., Cook, D.J., and Neville, A.S., 2015, Saqqar: A new 34 km diameter impact crater in Saudi Arabia: Meteoritics & Planetary Science, v. 50, no. 11, p. 1925–1940, https://doi.org/10.1111/maps.12555.

Kenkmann, T., Sundell, K.A., and Cook, D., 2018, Evidence for a large Paleozoic impact crater strewn field in the Rocky Mountains: Scientific Reports, v. 8, https://doi.org/10.1038/s41598-018-31655-4.

Kenkmann, T., Müller, L., Fraser, A., Cook, D., Sundell, K., and Rae, A.S.P., 2022, Secondary cratering on Earth: The Wyoming impact crater field: Geological Society of America Bulletin, v. 134, p. 2469–2484, https://doi.org/10.1130/B36196.1.

Koeberl, C., and Reimold, W.U., 1995, The Newporte impact structure, North Dakota, USA: Geochimica et Cosmochimica Acta, v. 59, p. 4747–4767, https://doi.org/10.1016/0016-7037(95)00339-8.

Langenhorst, F., and Deutsch, A., 1994, Shock experiments on pre-heated α- and β-quartz: II. X-ray and TEM investigations: Earth and Planetary Science Letters, v. 128, no. 3–4, p. 683–698, https://doi.org/10.1016/0012-821X(94)90179-1.

Langenhorst, F., Boustie, M., Deutsch, A., Hornemann, U., Matigon, Ch., Migault, A., and Romain, J.P., 2003, Experimental techniques for the simulation of shock metamorphism: A case study on calcite, *in* Davison, L., Horie, Y., and Sekine, T., eds., High-Pressure Shock Compression of Solids V: Shock Wave and High Pressure Phenomena: New York, Springer, p. 1–27, https://doi.org/10.1007/978-1-4613-0011-3_1.

Lawson, D.E., and Smith, J.R., 1966, Pennsylvanian and Permian influence on Tensleep oil accumulation, Big Horn Basin, Wyoming: American Association of Petroleum Geologists Bulletin, v. 50, no. 10, p. 2197–2220, https://doi.org/10.1306/5D25B719-16C1-11D7-8645000102C1865D.

Love, J.D., 1988, Geology of the Bighorn Basin, northern Wyoming and southern Montana, *in* Sloss, L.L., ed., Sedimentary Cover—North American Craton, U.S.: Geological Society of America, Decade of North American Geology: The Geology of North America, v. D-2, p. 201–204, https://doi.org/10.1130/DNAG-GNA-D2.109.

May, S.R., Gray, G.G., Summa, L.L., Stewart, N.R., Gehrels, G.E., and Pecha, M.E., 2013, Detrital zircon geochronology from the Bighorn Basin, Wyoming, USA: Implications for tectonostratigraphic evolution and paleogeography: Geological Society of America Bulletin, v. 125, p. 1403–1422, https://doi.org/10.1130/B30824.1.

McDonnell, A., Loucks, R.G., and Dooley, T., 2007, Quantifying the origin and geometry of circular sag structures in northern Fort Worth Basin, Texas: Paleocave collapse, pull-apart fault systems, or hydrothermal alteration?: American Association of Petroleum Geologists Bulletin, v. 91, no. 9, p. 1295–1318, https://doi.org/10.1306/05170706086.

Melosh, H.J., 1989, Impact Cratering: A Geologic Process: Oxford Monographs on Geology and Geophysics 11, 245 p.

Moore, D.A., 1984, The Tensleep Formation of the southeastern Bighorn Basin, Wyoming, *in* Goolsby, J., and Morton, D., eds., The Permian and Pennsylvanian Geology of Wyoming: Casper, Wyoming, Wyoming Geological Association, 35th Annual Field Conference Guidebook, p. 273–279.

Morgan, J.V., et al., 2016, The formation of peak rings in large impact craters: Science, v. 354, no. 6314, p. 878–882, https://doi.org/10.1126/science.aah6561.

Neely, T.G., and Erslev, E.A., 2009, The interplay of fold mechanisms and basement weaknesses at the transition between Laramide basement-involved arches, north-central Wyoming, USA: Journal of Structural Geology, v. 31, p. 1012–1027, https://doi.org/10.1016/j.jsg.2009.03.008.

Nicholson, U., Bray, V.J., Gulick, S.P.S., and Aduomahor, B., 2022, The Nadir Crater offshore West Africa: A candidate Cretaceous–Paleogene impact structure: Science Advances, v. 8, no. 33, https://doi.org/10.1126/sciadv.abn3096.

Ormö, J., 2015, Nested crater, *in* Hargitai, H., and Kereszturi, Á., eds., Encyclopedia of Planetary Landforms: New York, Springer, p. 1440–1444, https://doi.org/10.1007/978-1-4614-3134-3_515.

Ormö, J., and Lindström, M., 2000, When a cosmic impact strikes the sea bed: Geological Magazine, v. 137, no. 1, p. 67–80, https://doi.org/10.1017/S0016756800003538.

Passchier, C.W., and Trouw, R.A.J., 2005, Microtectonics: Berlin, Springer-Verlag, 366 p.

Pierce, W.G., 1966, Geologic Map of the Cody Quadrangle, Park County, Wyoming: U.S. Geological Survey Geologic Quadrangle Map GQ-542, scale 1:62,500, https://doi.org/10.3133/gq542.

Pierce, W.G., and Nelson, W.H., 1968, Geologic Map of the Pat O'Hara Mountain Quadrangle, Park County, Wyoming: U.S. Geological Survey Geologic Quadrangle Map GQ-0755, scale 1:62,500, https://doi.org/10.3133/gq755.

Poag, C.W., Koeberl, C., and Reimold, W.U., 2004, The Chesapeake Bay Crater—Geology and Geophysics of a Late Eocene Submarine Impact Structure: Heidelberg, Germany, Springer, Impact Studies Series, 522 p., https://doi.org/10.1007/978-3-642-18900-5.

Quaide, W.L., and Oberbeck, V.R., 1968, Thickness determinations of the lunar surface layer from lunar impact craters: Journal of Geophysical Research, v. 73, p. 5247–5270, https://doi.org/10.1029/JB073i016p05247.

Röller, K., and Trepmann, C.A., 2008, Stereo 32, Version 1.0.1: Bochum, Germany, Institut für Geologie, Mineralogie & Geophysik, Ruhr-Universität Bochum, http://www.ruhr-uni-bochum.de/hardrock/downloads.htmS.

Stewart, S., 1999, Seismic interpretation of circular geological structures: Petroleum Geoscience, v. 5, no. 3, p. 273–285, https://doi.org/10.1144/petgeo.5.3.273.

Stöffler, D., and Langenhorst, F., 1994, Shock metamorphism of quartz in nature and experiment: I. Basic observation and theory: Meteoritics, v. 29, no. 2, p. 155–181, https://doi.org/10.1111/j.1945-5100.1994.tb00670.x.

Stone, D., 1967, Theory of Paleozoic oil and gas accumulation in Bighorn Basin, Wyoming: American Association of Petroleum Geologists Bulletin, v. 51, no. 10, p. 2056–2114, https://doi.org/10.1306/5D25C1F7-16C1-11D7-8645000102C1865D.

Stone, D., and Therriault, A., 2003, Cloud Creek structure, central Wyoming, USA: Impact origin confirmed: Meteoritics & Planetary Science, v. 38, no. 3, p. 445–455, https://doi.org/10.1111/j.1945-5100.2003.tb00279.x.

Sturm, S., Wulf, G., Jung, D., and Kenkmann, T., 2013, The Ries impact, a double-layer rampart crater on Earth: Geology, v. 41, p. 531–534, https://doi.org/10.1130/G33934.1.

Sundell, K.A., 1990, Sedimentation and tectonics of the Absaroka Basin of northwestern Wyoming, *in* Specht, R.W., eds., Wyoming Sedimentation and Tectonics: Casper, Wyoming, Wyoming Geological Association, 41st Field Conference Guidebook, p. 105–122.

Sundell, K.A., 1993, A geologic overview of the Absaroka volcanic province, *in* Snoke, A.W., Steidtman, J.R., and Roberts, S.M., eds., Geology of Wyoming: Geological Survey of Wyoming Memoir 5, p. 480–506.

Todd, T.W., 1964, Petrology of Pennsylvanian rocks, Bighorn Basin, Wyoming: American Association of Petroleum Geologists Bulletin, v. 48, no. 7, p. 1063–1090, https://doi.org/10.1306/BC743D77-16BE-11D7-8645000102C1865D.

Science Editor: Mihai Ducea
Associate Editor: Christian Koeberl

Manuscript Received 1 June 2023
Revised Manuscript Received 21 November 2023
Manuscript Accepted 8 January 2024